AFRL-AFOSR-VA-TR-2016-0330

Optimizing Glassy Polymer Network Morphology for Nano-particle Dispersion, Stabilization

Jeffrey Wiggins
UNIVERSITY OF SOUTHERN MISSISSIPPI
2609 W 4TH ST STE H
HATTIESBURG, MS 39401

10/03/2016
Final Report

Air Force Research Laboratory
AF Office Of Scientific Research (AFOSR)/RTA1

REPORT DOCUMENTATION PAGE

Form Approved
OMB No. 0704-0188

PLEASE DO NOT RETURN YOUR FORM TO THE ABOVE ORGANIZATION.

1. REPORT DATE *(DD-MM-YYYY)*	2. REPORT TYPE	3. DATES COVERED *(From - To)*
20-05-2016	Final Report	March 1, 2013 to February 28, 2016

4. TITLE AND SUBTITLE
Optimizing Glassy Polymer Network Morphology for Nano-Particle Dispersion, Stabilization and Performance

5a. CONTRACT NUMBER
FA-13-1-0103

5b. GRANT NUMBER
GR04775

5c. PROGRAM ELEMENT NUMBER
NA

6. AUTHOR(S)
Jeffrey Wiggins

5d. PROJECT NUMBER
NA

5e. TASK NUMBER
NA

5f. WORK UNIT NUMBER
NA

7. PERFORMING ORGANIZATION NAME(S) AND ADDRESS(ES)
University of Southern Mississippi
Box 5157
118 College Drive
Hattiesburg, MS 39406

8. PERFORMING ORGANIZATION REPORT NUMBER
NA

9. SPONSORING/MONITORING AGENCY NAME(S) AND ADDRESS(ES)
USAF, AFRL DUNS 143574726
AF Office of Scientific Research
875 North Randolph Street, RM 3112
Arlington, VA 22203

10. SPONSOR/MONITOR'S ACRONYM(S)
AFOSR

11. SPONSOR/MONITOR'S REPORT NUMBER(S)

12. DISTRIBUTION/AVAILABILITY STATEMENT
DISTRIBUTION A: Distribution approved for public release.

13. SUPPLEMENTARY NOTES
NA

14. ABSTRACT
MWCNT nanocomposite aerospace prepolymers were successfully prepared in a one-step high volume process through the development of a new preparation approach based upon a high-shear continuous reaction method. The continuous reactor based upon two principle advancements in process engineering.
1. Chain extension prepolymer reactions including curative dissolution, toughener dissolution and controlled chain-extension reactions in the continuous reactor high temperature “hot-zone” to advance conversion, rheology and tack.
2. Simultaneous MWCNT dispersion and stabilization in the continuous reactor low temperature “cold-zone” leading to an increased viscosity and stabilization of MWCNTs within rheological regimes which inhibit re-agglomeration to aid in post processing stabilization of dispersion state through final cure.
The significance of this work is the demonstration of a new method to prepare fully dispersed MWCNT aerospace prepolymers, from reactants to fi

15. SUBJECT TERMS
MWCNT; Multifunctional Composite
Continuous Reactor Aerospace Prepolymer
Prepreg

16. SECURITY CLASSIFICATION OF:			17. LIMITATION OF ABSTRACT	18. NUMBER OF PAGES	19a. NAME OF RESPONSIBLE PERSON
a. REPORT	b. ABSTRACT	c. THIS PAGE			Jeffrey Wiggins
NA	NA	NA	NA	70	19b. TELEPHONE NUMBER *(Include area code)* 601-266-6960

Reset

INSTRUCTIONS FOR COMPLETING SF 298

1. REPORT DATE. Full publication date, including day, month, if available. Must cite at least the year and be Year 2000 compliant, e.g. 30-06-1998; xx-06-1998; xx-xx-1998.

2. REPORT TYPE. State the type of report, such as final, technical, interim, memorandum, master's thesis, progress, quarterly, research, special, group study, etc.

3. DATES COVERED. Indicate the time during which the work was performed and the report was written, e.g., Jun 1997 - Jun 1998; 1-10 Jun 1996; May - Nov 1998; Nov 1998.

4. TITLE. Enter title and subtitle with volume number and part number, if applicable. On classified documents, enter the title classification in parentheses.

5a. CONTRACT NUMBER. Enter all contract numbers as they appear in the report, e.g. F33615-86-C-5169.

5b. GRANT NUMBER. Enter all grant numbers as they appear in the report, e.g. AFOSR-82-1234.

5c. PROGRAM ELEMENT NUMBER. Enter all program element numbers as they appear in the report, e.g. 61101A.

5d. PROJECT NUMBER. Enter all project numbers as they appear in the report, e.g. 1F665702D1257; ILIR.

5e. TASK NUMBER. Enter all task numbers as they appear in the report, e.g. 05; RF0330201; T4112.

5f. WORK UNIT NUMBER. Enter all work unit numbers as they appear in the report, e.g. 001; AFAPL30480105.

6. AUTHOR(S). Enter name(s) of person(s) responsible for writing the report, performing the research, or credited with the content of the report. The form of entry is the last name, first name, middle initial, and additional qualifiers separated by commas, e.g. Smith, Richard, J, Jr.

7. PERFORMING ORGANIZATION NAME(S) AND ADDRESS(ES). Self-explanatory.

8. PERFORMING ORGANIZATION REPORT NUMBER. Enter all unique alphanumeric report numbers assigned by the performing organization, e.g. BRL-1234; AFWL-TR-85-4017-Vol-21-PT-2.

9. SPONSORING/MONITORING AGENCY NAME(S) AND ADDRESS(ES). Enter the name and address of the organization(s) financially responsible for and monitoring the work.

10. SPONSOR/MONITOR'S ACRONYM(S). Enter, if available, e.g. BRL, ARDEC, NADC.

11. SPONSOR/MONITOR'S REPORT NUMBER(S). Enter report number as assigned by the sponsoring/ monitoring agency, if available, e.g. BRL-TR-829; -215.

12. DISTRIBUTION/AVAILABILITY STATEMENT. Use agency-mandated availability statements to indicate the public availability or distribution limitations of the report. If additional limitations/ restrictions or special markings are indicated, follow agency authorization procedures, e.g. RD/FRD, PROPIN, ITAR, etc. Include copyright information.

13. SUPPLEMENTARY NOTES. Enter information not included elsewhere such as: prepared in cooperation with; translation of; report supersedes; old edition number, etc.

14. ABSTRACT. A brief (approximately 200 words) factual summary of the most significant information.

15. SUBJECT TERMS. Key words or phrases identifying major concepts in the report.

16. SECURITY CLASSIFICATION. Enter security classification in accordance with security classification regulations, e.g. U, C, S, etc. If this form contains classified information, stamp classification level on the top and bottom of this page.

17. LIMITATION OF ABSTRACT. This block must be completed to assign a distribution limitation to the abstract. Enter UU (Unclassified Unlimited) or SAR (Same as Report). An entry in this block is necessary if the abstract is to be limited.

EXECUTIVE SUMMARY

Significant Aerospace Composite Research Accomplishments (Award Period)

1. Matrix Continuous Prepolymer Reactor Developed (**Page 4**)
2. Nano-Matrix Continuous Prepolymer Reactor Developed (**Page 22**)
3. Nano-Matrix Prepreg Process Developed (**Page 45**)
4. Cured Nanostructured Matrix Morphologies Developed (**Page 52**)
5. Benzoxazine Matrix Continuous Reactor Developed (**Page 62**)

Significant Aerospace Professional Development (Award Period)

1. Dr. Katherine Frank, Boeing Research and Technology (2013)
    a. Ph.D. Dissertation: *Relationships between cure kinetics, network architecture, and fluid sensitivity in Glassy Epoxy Networks*
2. Dr. Jinwei Tu; WRG Laboratory Manager (2013)
    a. Ph.D. Dissertation: *Investigation of glassy state molecular motions in thermoset polymers*
3. Dr. David Kingsley, GE Aviation (2014)
    a. Ph.D. Dissertation: *Continuous prepolymer reactor design*
4. Dr. Christopher Childers, Boeing Research and Technology (2014)
    a. Ph.D. Dissertation: *Relating macromolecular behavior to molecular structure in composite matrix polymers*
5. Dr. Xiaole Cheng, Corning (2015)
    a. Ph.D. Dissertation: *Cure kinetics, morphologies and mechanical properties of thermoplastic/MWCNT modified multifunctional glassy epoxies prepared via continuous reaction methods*
6. Dr. Jeremy Moskowitz, Cytec Aerospace Materials (2015)
    a. Ph.D. Dissertation: *Polyacrylonitrile copolymers: Effects of molecular weight, polydispersity, composition and sequencing on thermal ring-closing stabilization*
7. Dr. John Misasi, Western Washington University Composites Engineering Faculty (2015)
    a. Ph.D. Dissertation: *Hybrid Aryl-etherketone and hyperbranched epoxy networks*

Relevant Refereed Publications (Award Period)

i. *Molecular scale cure rate dependence of thermoset matrix polymers,* Childers, Christopher, Hassan, Mohammad, Mauritz, Kenneth, Wiggins, Jeffrey, *Arabian Journal of Chemistry* **2016,** 9, 206
ii. *Semibatch RAFT copolymerization of acrylonitrile and N-isopropylacrylamide: Effect of comonomer distribution on cyclization and thermal stability*, Moskowitz, Jeremy and Wiggins, Jeffrey, *Polymer* **2016,** 84, 311

iii. *Thermo-oxidative stabilization of polyacrylontirile and its copolymers: Effect of molecular weight, dispersity and polymerization pathway*, Moskowitz, Jeremy and Wiggins, Jeffrey, *Polymer Degradation and Stability* **2016,** 125, 76
iv. *High Molecular Weight and Low Dispersity Polyacrylonitrile by Low Temperature RAFT Polymerization*, Moskowitz, Jeremy, Abel, Brooks, McCormick, Charles, Wiggins, Jeffrey, *J. Poly. Sci. Pt.A – Poly Chem,* **2016,** 54, 553
v. *Polymer chain dynamics in epoxy based nanocomposites as investigated by broadband dielectric spectroscopy*, Hassan, Mohammad, Tucker, Samuel, Abukmail, Ahmed, Wiggins, Jeffrey, Mauritz, Kenneth, *Arabian Journal of Chemistry* **2016,** 9, 203
vi. *Digital image correlation analysis of strain recovery in glassy polymer network isomers*, Stephen Heinz, Jianwei Tu, Matthew Jackson, Jeffrey Wiggins, *Polymer* **2016,** 82, 87
vii. *Ductile thermoset polymers by controlling network flexibility*, Hameed, Nishar, Fox, Bronwyn, Salim, Nisa, Walsh, Tiffany, Wiggins, Jeffrey *Chem. Comm.* **2015,** 51, 9903
viii. *Simultaneous reinforcement and toughness improvement in an aromatic epoxy network with an aliphatic hyperbranched POSS epoxy modifier*, Jin, Qingfen, Misasi, John, Wiggins, Jeffrey, Morgan, Sarah ", *Polymer,* **2015** 73, 174

ix. *Phenylene ring motions in isomeric glassy epoxy networks and their contributions to thermal and mechanical properties*, Tu, Jinwei, Tucker, Samuel, Christensen, Stephen, Sayed, Abdelwahed, Jarrett, William, Wiggins, Jeffrey, **2015** *Macromolecules*, 48(6), 1748
x. *Surface composition control via chain end segregation in polyethersulfone solution cast films*, Knauer, Katrina, Greenhoe, Brian, Wiggins, Jeffrey, Morgan, Sarah **2015** *Polymer*, 57(28), 88
xi. *Laser-induced thermo-oxidative degradation of carbon nanotube/polypropylene nanocomposites*, Bartolucci, Stephen, Supan, Karen, Warrender, Jeffrey, Davis, Christopher, La Beaud, Lawrence, Knowles, Kyler, Wiggins, Jeffrey **2014** *Composites Science and Technology*, 105, 166
xii. *Continuous reactor preparation of thermoplastic modified epoxy-amine prepolymers*, Cheng, Xiaole, Wiggins, Jeffrey **2014** *Polymer International*, 63(10) 1777
xiii. *Thermal stability of polypropylene-clay nanocomposites subjected to laser pulse heating* Bartolucci, Stephen, Supan, Karen, Wiggins, Jeffrey, LaBeaud, Lawrence, Warrender, Jeffrey **2013** *Polymer Degradation and Stability* 98(12) 2497

Relevant Reviewed Publications and Presentations (Award Period)

i. *Effect of Molecular Weight and Polydispersity on Thermal Ring-Closing Stabilization (Cyclization) of Polyacrylonitrile.* Katelyn Cordell, Jeremy Moskowitz, Jeffery Wiggins, Society for the Advancement of Material and Process Engineering, CAMX International Symposium Proceedings, Dallas, TX, October 2015

ii. *Dispersion of MWCNTs in an Epoxy Prepolymer Matrix Via Continuous Reactor Processing.* Andrew Frazee, Jeffrey Wiggins, Society for the Advancement of Material and Process Engineering, CAMX International Symposium Proceedings, Dallas, TX, October 2015
iii. *Quantitative Analysis of the Effect of Ramp Rate on Network Formation during the Cure of TGDDM-DDS Matrices Using Near-Infrared Spectroscopy.* Andrew Janisse, Jeffrey Wiggins, Society for the Advancement of Material and Process Engineering, CAMX International Symposium Proceedings, Dallas, TX, October 2015
iv. *Effect of Epoxy Molecular Weight on Incorporation of Polyhedral Oligomeric Silsesquioxane (POSS) as Pendant cage in Epoxy-POSS Hybrid Networks.* Amit Sharma, Jeffery Wiggins, Society for the Advancement of Material and Process Engineering, CAMX International Symposium Proceedings, Dallas, TX, October 2015
v. *Manipulation of cure prescription to alter nano-morphology of dispersed multiwall carbon nanotubes.* Brian Greenhoe, Jeffrey Wiggins, Society for the Advancement of Material and Process Engineering, CAMX International Symposium Proceedings, Dallas, TX, October 2015
vi. *Observing Residual strains in carbon fiber composites laminates with digital image correlation.* Kyler Knowles, Jeffrey Wiggins, Society for the Advancement of Material and Process Engineering, CAMX International Symposium Proceedings, Dallas, TX, October 2015 (2nd Place Technical Recognition)
vii. *Improving Polymer Composite Matrix Toughness with POSS-Modified Hyperbranched epoxies.* John Misasi, Sarah Morgan, Jeffrey Wiggins, Society for the Advancement of Material and Process Engineering, CAMX International Symposium Proceedings, Dallas, TX, October 2015
viii. *Improcessabilty of Thermoplastic PEEK composites via Ring Opening Polymerization.* Matthew Patterson, John Misasi, Jeffrey Wiggins, Russell Varley, Society for the Advancement of Material and Process Engineering, CAMX International Symposium Proceedings, Dallas, TX, October 2015
ix. *Development of Layered POSS Epoxy-Amine Nanocomposites for Protective Coatings* Jessica Piness, Jeffrey Wiggins, CAMX 2015, Dallas, TX October 2015
x. *Atomic Oxygen Exposure Testing of Novel Layered POSS Thermoset Nanocomposites* Jessica Piness, Katrina Knauer, Jeffrey Wiggins, International Astronautical Congress, Jerusalem, Israel, October 2015
xi. *Ultraviolet Exposure Testing of Novel POSS-Cerium Oxide Thermoset Nanocomposites* Jessica Piness, Katrina Knauer, Jeffrey Wiggins, AIAA Space, Pasadena, CA August 2015
xii. *Atomistic and Macro-scale Mechanical Property Testing of POSS Nanocomposites for Space Applications* Jessica Piness, Katrina Knauer, Jeffrey Wiggins, SAMPE Tech 2015, Baltimore, MD, May 2015
xiii. *Cure behavior and polymer chain dynamics of octaphenyl poss-epoxy-amine networked systems via dielectric spectroscopy and dynamic mechanical analysis techniuqes,* Jessica Piness, Mohamed Hassan, Jeffrey Wiggins, Society for the Advancement of Material and Process Engineering, International Symposium Proceedings, Orlando, FL, October 2014

xiv. *Controlled polyacrylonitrile precursor chemistries*, Jeremy Moskowitz, Brooks Abel, Charles McCormick, Jeffrey Wiggins, Society for the Advancement of Material and Process Engineering, International Symposium Proceedings, Orlando, FL, October 2014
xv. *Dispersion and stabilization of MWCNT in epoxy prepolymer matrix using continuous reactor,* Xiaole Cheng, Brian Greenhoe, Mohamed Hassan, Jeffrey Wiggins, Society for the Advancement of Material and Process Engineering, International Symposium Proceedings, Orlando, FL, October 2014
xvi. *Exploring MWCNTs agglomerate morphology control in epoxy matrix for gains in electrical properties*, Brian Greenhoe, Xiaole Cheng, Jeffrey Wiggins, Society for the Advancement of Material and Process Engineering, International Symposium Proceedings, Orlando, FL, October 2014
xvii. *Network formation dependence on polymer matrix cure rate,* Christopher Childers, Mohammed Hassan, Jeffrey Wiggins, Society for the Advancement of Material and Process Engineering, International Symposium Proceedings, Seattle, WA, June 2014
xviii. *Network conversion studies of poss-epoxy-amine nanocomposites,* Jessica Piness, Jeffrey Wiggins, Society for the Advancement of Material and Process Engineering, International Symposium Proceedings, Seattle, WA, June 2014

SUMMARY OF RESEARCH ACCOMPLISHMENTS

1. Aerospace Composite Matrix Continuous Prepolymer Reactor Developed

Preliminary research conducted in this research required our research group to develop a "new-to-the-world" approach for preparing composite matrix chemistries. Traditional methods for batch reactions of typical aerospace matrix prepolymers are low shear reactors which are incapable of properly dispersing nanoparticles. And, traditional methods for dispersing nanoparticles within aerospace prepolymers are traditionally based upon sonication techniques and solvents which are impractical for real-world applications. One of our primary project hypotheses was to develop a high-shear continuous reactor, based upon 100% solids to simultaneously prepare aerospace prepolymers and disperse nanoparticles. This portion of our report describes a new high-shear continuous reactor method to prepare thermoplastic modified epoxy prepolymers for aerospace prepregs with the aim of replacing traditional batch reactors. In order to proceed in our

research, we felt it was important to demonstrate our ability to prepare aerospace prepolymers in the continuous reactor and prove the reaction product was similar to those prepared by the traditional batch process. Compared to batch reactors, the continuous reactor is capable of producing epoxy prepolymers through simultaneous dissolution of polyethersulfone (PES) and 4, 4' - diaminodiphenylsulfone (44DDS) in tetraglycidyl - 4, 4' - diaminodiphenylmethane (TGDDM). Chemical structures are shown in Figure 1.

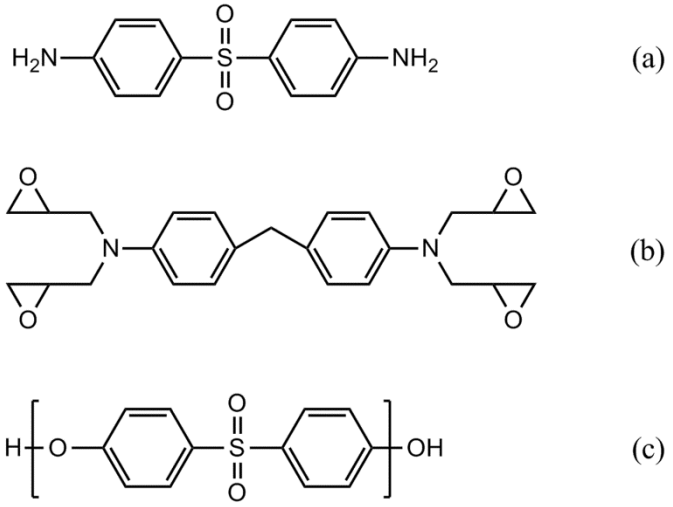

Figure 1. (a) 44DDS, (b) TGDDM, and (c) PES

In addition, concurrent chain extension reactions advance prepolymer molecular weights to desired viscosities in less than 2 minutes of mean residence time. Optical micrographs were used to define how process temperature influences PES dissolution in TGDDM in continuous reactor. Kinetic studies confirmed the chain extension reaction in continuous reactor is similar to batch reactor, and the molecular weights and viscosities of prepolymers were readily controlled through reaction kinetics. Atomic force microscopy was used to confirm similar cured network morphologies for formulations prepared from batch and continuous reactors. Additionally tensile

strength, tensile modulus and fracture toughness analyses concluded mechanical properties of cured epoxy matrices produced from both reactors were equivalent.

The continuous reaction was accomplished using a Prism 16 mm co-rotating intermeshing twin-screw extruder (L/D = 25). The reactor consists of a feed zone, five electrical heated and liquid cooled zones, and an electrical heated die zone (Figure 2). The screw configuration shown in Figure 2 was designed to balance shear mixing and residence time with a combination of various conveying, kneading and reverse elements. The reaction screws were optimized using three sections of kneading blocks to provide adequate shear mixing. Reverse elements were incorporated in Zone 3 to optimize the residence time, generate back-pressure and promote the chain-extension reaction.

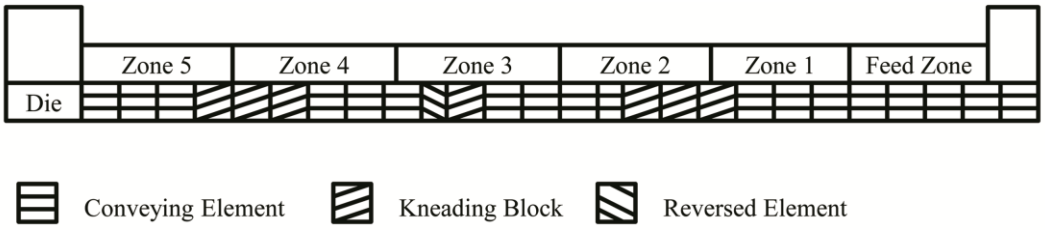

Figure 2. Screw configuration of the aerospace matrix high-shear continuous reactor

The preparation of TGDDM/44DDS/PES prepolymers and cured networks creates a complex physical and chemical environment including dissolution of PES and 44DDS in TGDDM, chain extension reactions or cure reactions of TGDDM/44DDS/PES, and ultimately the reaction induced phase separation of PES in TGDDM/44DDS matrix during cure. This research provides a direct comparison of these processes for batch and continuous reactors to determine the utility of continuous reactors for preparing aerospace prepreg epoxy prepolymers.

Thermoplastic modified epoxy-amine prepolymers are prepared in batch reactors in two steps. First, thermoplastics are dissolved into epoxides at 120 °C to 150 °C over a relatively long period of time until fully dissolved. Once dissolved, temperatures are adjusted for amine dissolution and prepolymer is advanced to prescribed molecular weights and viscosities. Herein, we report 120 °C for dissolution of PES and 44DDS to simplify our analysis. Figure 3 shows optical micrographs for PES dissolved in TGDDM at 120 °C for 10 min, 30 min, 50 min, and 70 min from a batch reactor. Percentages of undissolved PES area (P) quantified by image software were used to depict the progression of PES dissolution under these conditions. In this example 22.2 % of PES particles were undissolved at 10min and 0.3 % at 70 min, suggesting dissolution progresses with dissolution time. We determined 5 wt% PES to be fully dissolved in TGDDM after 70 min in the batch reactor at 120 °C.

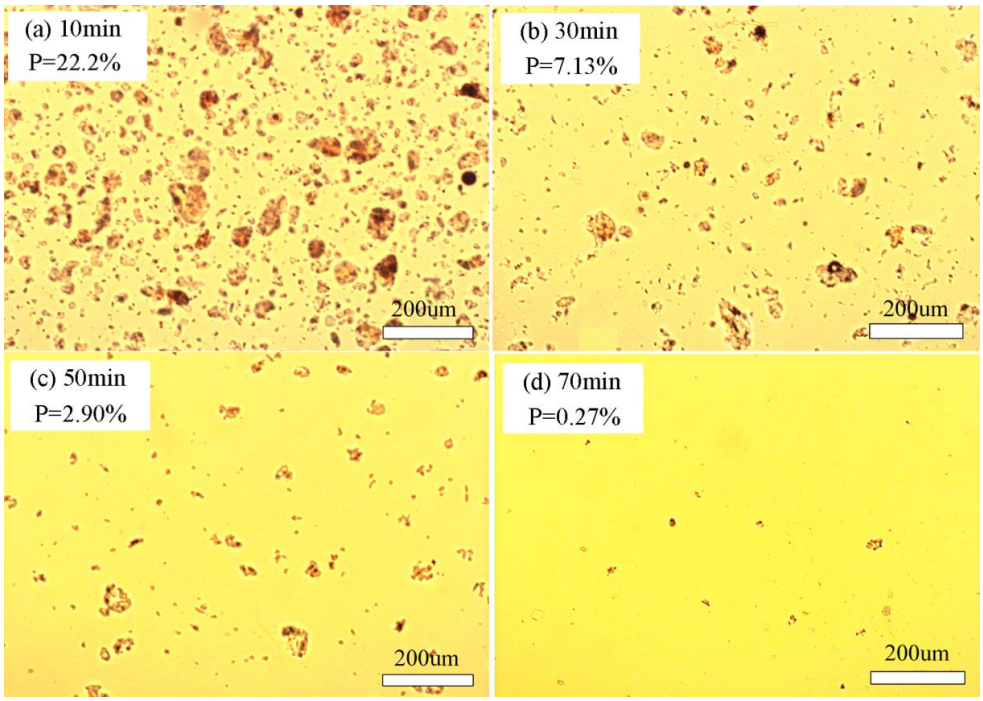

Figure 3. Batch reactor dissolution states at 120°C

Upon PES dissolution in the batch reactor 44DDS was added to the TGDDM/PES mixture and chain extension reactions were started until prescribed molecular weights and viscosities achieved. Reaction kinetics was measured using DSC through a series of isothermal experiments to quantify cure conversions. Figure 4 describes conversion vs. time of TGDDM/44DDS/PES reactions at various temperatures which displaying two distinct regions. The first region in the early stages was kinetically controlled characterized by a rapid rate of reaction. The second region was diffusion controlled described by a slower rate of reaction as the matrix vitrified. To model the progress of cure reaction, diffusion was considered and we employed an autocatalytic expression proposed by Chen and Macosko[15] (Eq. 1 and 2) to describe our reaction behaviors.

$$\frac{d\alpha}{dt} = (k_1 + k_2\alpha^m)(1-\alpha)^{n_1}; \quad \alpha < \alpha_d \qquad \text{(Eq.1)}$$

$$\frac{d\alpha}{dt} = k_3(\alpha_p - \alpha)^{n_2}; \quad \alpha > \alpha_d \qquad \text{(Eq.2)}$$

where k_1, k_2, and k_3 are the kinetic rate constants, m, n_1 and n_2 are the kinetic exponents of the cure reactions, α_p is the maximum degree of conversion, and α_d is the maximum of the derivative of the curve from the cure reaction rate as function of conversion describing the onset of the diffusion controlled reaction.

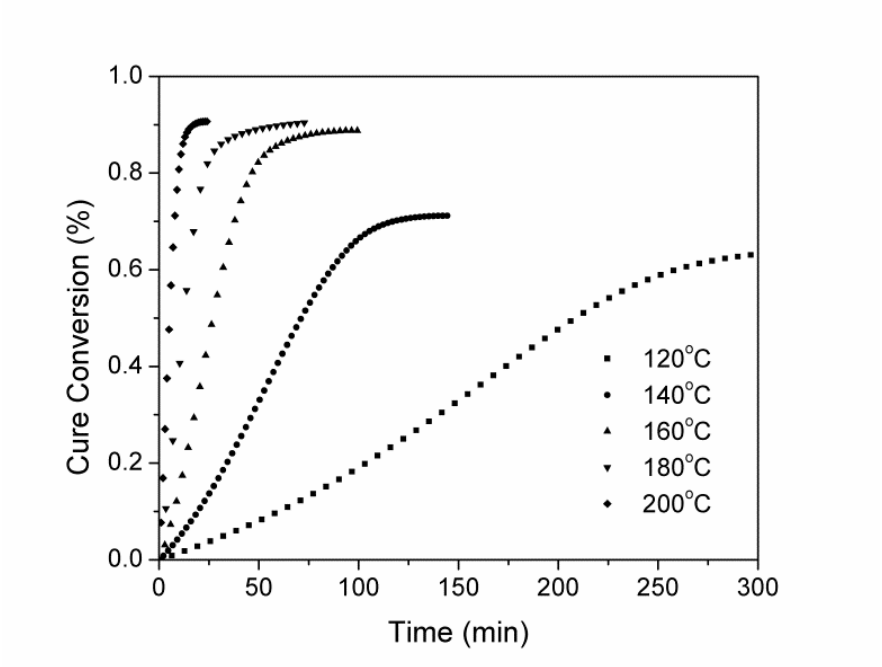

Figure 4. Cure conversion vs. reaction time at different curing temperatures

The cure model parameters were obtained simultaneously by applying a multiply regression method to calculate the data and provided in Table 1. The overall TGDDM/44DDS/PES reaction order for kinetic controlled reaction, $m+n_1$, was approximately 2.5, while the reaction order for diffusion controlled reaction was approximately 1.0. The rate constants k_1, k_2, and k_3 increased with temperature and k_2 was greater than k_1. The rate constants were temperature dependent and we calculated Arrhenius relationships between lnk_1, lnk_2, lnk_3, vs. $1/T$ described in Figure 5. The activation energies for $E_{a,1}$, $E_{a,2}$, and $E_{a,3}$ were calculated as 74.0, 63.2, and 55.0 kJ mol^{-1}, respectively. These results agree well with those reported for similar epoxy systems.[16]

Table 1. Kinetic and diffusion control parameters for TGDDM/44DDS/PES batch reaction

Temperature (°C)	Kinetic control parameters				Diffusion control parameters	
	m	n_1	k_1	k_2	n_2	k_3
120	1.18	1.51	0.00138	0.0150	0.76	0.0114
140	1.02	1.43	0.00418	0.0324	0.68	0.0244
160	0.96	1.41	0.00995	0.0829	0.91	0.0600
180	1.05	1.45	0.0251	0.186	0.91	0.0900
200	1.01	1.53	0.0653	0.359	1.09	0.211

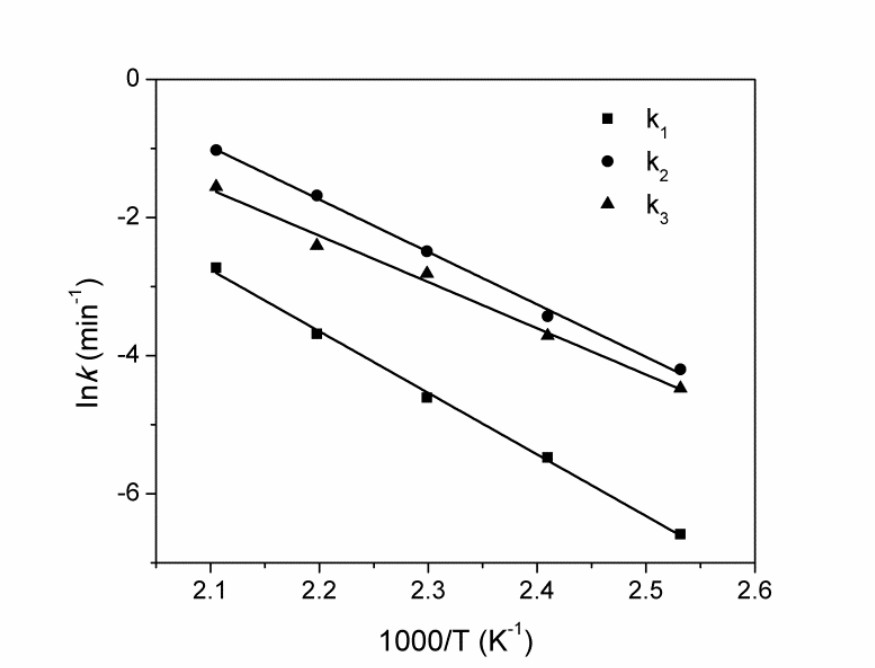

Figure 5. Arrhenius Plot of the rate constants for the cure reaction

Integration of Eq.5 and Eq.6 provides a description of cure conversion as a function of cure time. Figure 6 shows how the experimental values agreed with the model for the batch reaction at 120 °C. The experimental data fit well showing good accuracy of applying the autocatalytic model for TGDDM/44DDS/PES cure reactions in a batch reactor.

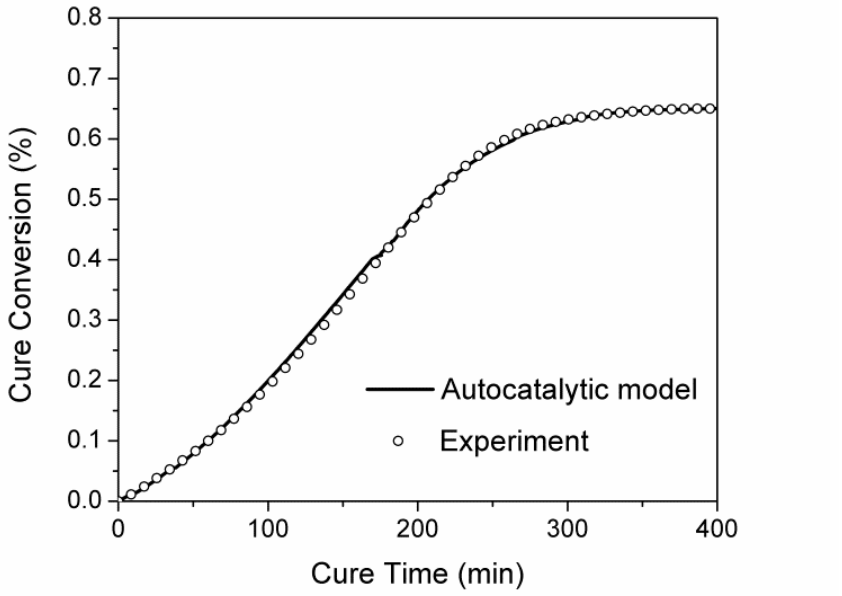

Figure 6. Calculated vs. experimental TGDDM/44DDS/PES conversion at 120 °C

When developing epoxy prepolymers for prepreg filming, prepolymer viscosity is varied for various impregnation strategies; modeling cure kinetics provides an ability to control prepolymer viscosity with temperature and reaction time. For the purpose of demonstration, a Brookfield viscosity of 20 Pa s at 80 °C is required for TGDDM/44DDS/PES prepolymers products based on our prepreg manufacturing experience. Figure 7 shows the cure conversion and the corresponding viscosity of TGDDM/44DDS/PES prepolymers as function of reaction time in

batch reactor. In this prepolymer reaction example, a Brookfield viscosity of 20 Pa s at 80 °C is observed at around 16 % cure conversion and 87min reaction time. Quantification of the relationships between temperature, conversion and viscosity derived through batch reactor experimentation will be critical for understanding epoxy prepolymer continuous reactors.

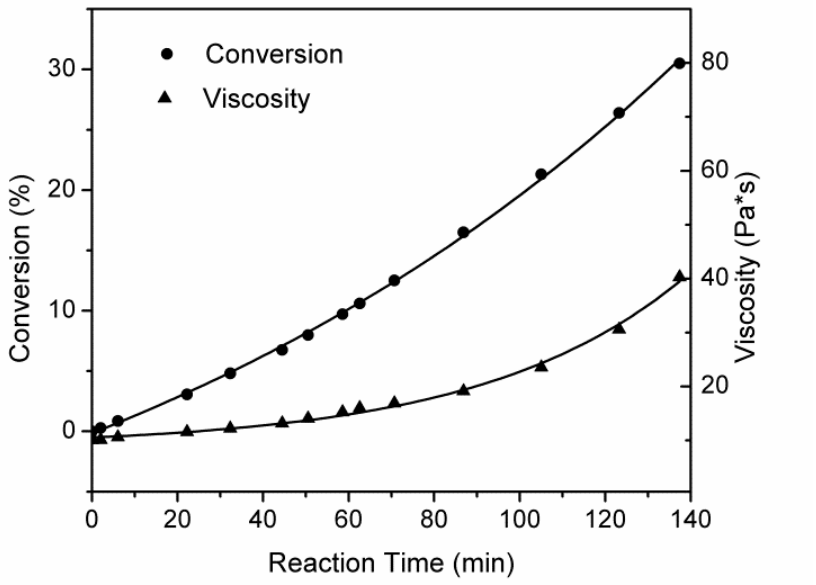

Figure 7. Conversion and 80 ^{o}C Brookfield viscosity of TGDDM/44DDS/PES prepolymers

Prepolymer continuous reaction

The prior discussion is provided to review conventional batch reactor epoxy prepolymer development protocols, highlight critical control variables, and benchmark necessary prepolymer properties for utility in advanced composites prepreg preparation. While batch reactors are generally based upon relatively low-temperature reactions over long periods of time, continuous reactors are designed for higher temperature reactions over short periods of time. Residence time

distribution in a continuous reactor is controlled through screw configuration, screw speed, feeding rate and reactor length, and is typically in the range of 1 to 5 min. Since residence time is low, reaction quantities are small and heat transfer efficiencies are high, continuous reactors offer a distinct advantage over batch reactors for controlling dissolution and cure reactions using elevated temperature.

The residence time distribution (RTD) and mean residence time ($\overline{t_m}$) were first measured to describe the history of materials within the continuous reactor. Figure 8 shows the RTD curve at a fixed operating condition of 300 rpm screw speed and 2.25 kg h^{-1} feed rate. The mean residence time was calculated to be approximately 2 min according to Eq.2. Conducting similar experiments over a range of temperatures confirmed mean residence time and distribution to be independent of process temperature for our system.

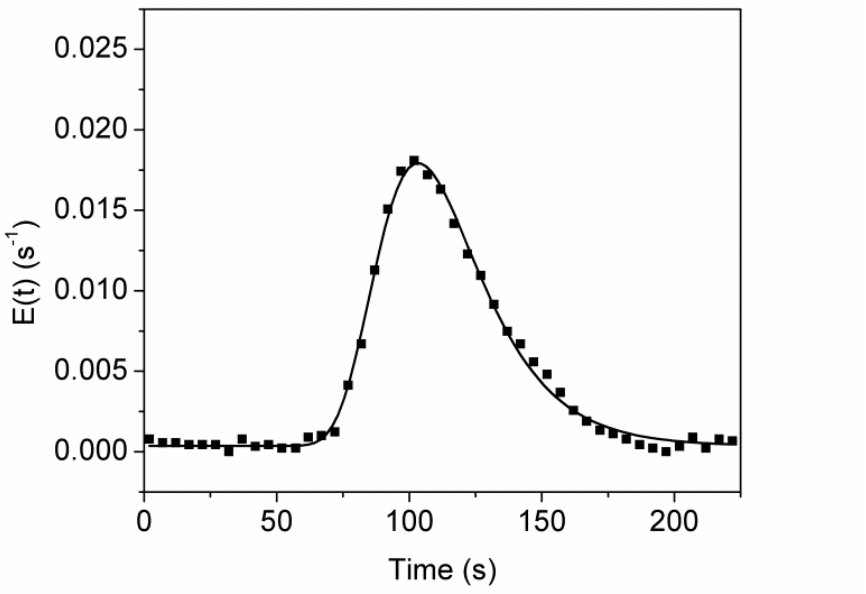

Figure 8. Continuous reactor RTD (solid line is best fit)

Figure 9 shows optical micrographs describing the effect of continuous reactor process temperature (120 °C - 180 °C) on dissolution states of PES in TGDDM. Comparison of 120 °C/2 min continuous reactor dissolution data in Figure 9a with 120 °C/10 min batch reactor data in Figure 3a depicts specific advantages of the continuous reactor over batch processes. This direct comparison highlights the continuous reactor efficiency in mixing and dissolution attributed to the increased shear, improved heat-transfer and reduced volume. Furthermore, the percentage of undissolved PES area in the continuous reactor was readily reduced within the 2 min residence time through increasing reactor temperature. Figure 9d shows the PES is fully dissolved in TGDDM at 180 °C to less than 1 % PES left. When comparing this result to the 120 °C/70 min batch reactor data provided in Figure 3d a marked potential to reduce dissolution time in the continuous reactor by elevated temperature is feasible. From these comparisons, it is obvious that mixing and dissolution through increasing temperature is more efficient in the continuous reactor since similar levels of dissolution states are achieved at significantly less times.

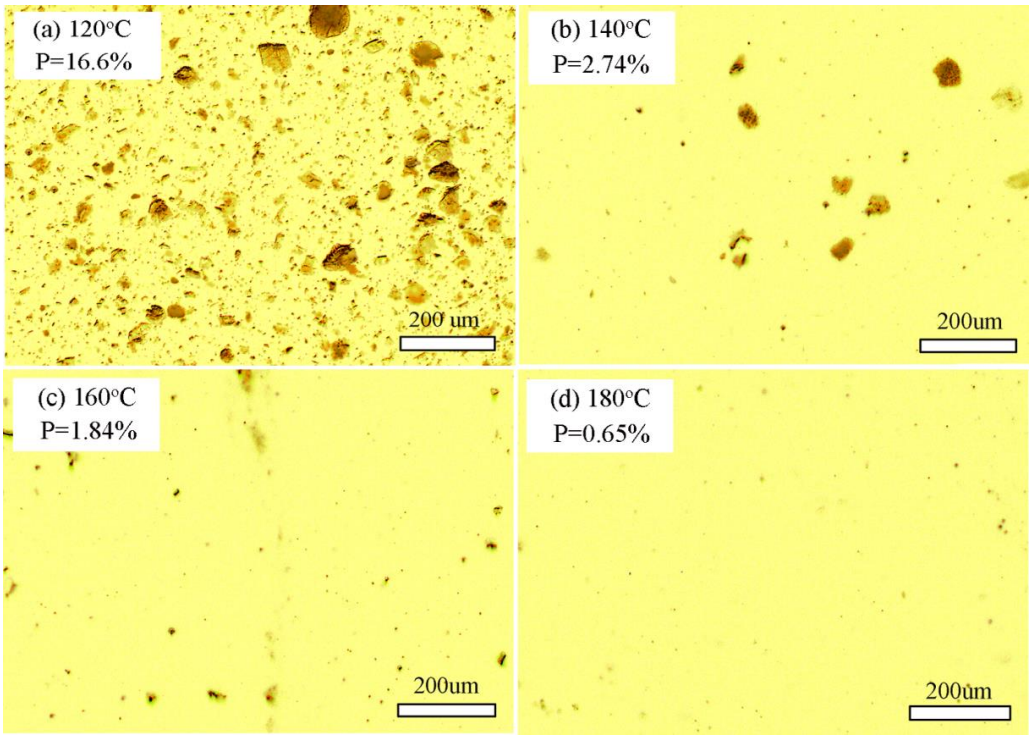

Figure 9. Continuous reactor dissolution states at various temperatures

Although temperature can be increased to reduce PES dissolution time in a batch reactor, it is impractical to control 44DDS dissolution and chain extension reaction at high temperatures and avoids gelation considering the large volume of batch reactors. Small reaction volumes and excellent heat transfer in continuous reactors provide pathways for using elevated temperatures to prepare epoxy prepolymers with reduced reaction time. But the challenge for avoiding gelation in a continuous reactor at high temperatures remains a critical problem. We have found predictive modeling of chain extension reactions is necessary for establishing continuous reactor conditions. The Total Segregation Model described by J.H. Ramirez[17] is useful for predicting reaction conversion to avoid gelation in the continuous reactor. This model shown in Eq.3 assumes that at steady state all reactants along the continuous reactor follow the residence time distribution $E(t)$ and the mean conversion ($\overline{x_m}$) is calculated through a series of discrete conversion states.

$$\overline{x_m} = \sum_0^\infty x_{batch}(t) \cdot E(t) \cdot \Delta t \qquad \text{(Eq.3)}$$

In the Total Segregation Model, $x_{batch}(t)$ is calculated from the kinetic model described in Eq.5 through the batch reaction analyses. The mean conversion at a given temperature for the continuous reactor was calculated using Eq.5 and Eq.7 and the results are presented in Table 2. It can be seen that the reaction is maintained at a relatively low conversion below 160 °C within our reactor setup. As the temperature is increased to 180°C, conversion increases exponentially with temperature. The predicted conversion is 42.3 % at 220 °C which is in the region of gelation, so we would use 200 °C as the maximum processing temperature for experimentation of continuous reaction.

Reaction conversions, viscosities and T_gs of TGDDM/44DDS/PES prepolymers prepared by continuous reactor at different process temperatures were measured experimentally and the results are provided in Table 2. 80 °C Brookfield viscosity of TGDDM/44DDS/PES prepolymers was measured at 20.3 Pa s for the 180 °C continuous reaction which displays good processability for preparing prepreg film and fiber-impregnation. T_gs of TGDDM/44DDS/PES prepolymers prepared from continuous reaction were in good agreement with similar conversions observed for batch reactor systems. This result suggests reaction conversions of prepolymers prepared by the continuous reactor were similar to those obtained through batch reactions.

Table 2. Predicted and experimental data for TGDDM/44DDS/PES prepolymers

Temperature (°C)	Predicted Conversion (%)	Experimental Conversion (%)	Experimental Viscosity (Pa s)	Experimental T_g (°C)
120	0.3	0.35	10.5	6.5
140	1.2	2.1	12.9	8.2
160	2.5	3.9	16.3	9.6
180	6.9	7.8	20.3	12.1
200	18.8	14.4	28.0	16.0
220	42.3	N/A	N/A	N/A

Figure 10 compares the experimental conversion data of prepolymer continuous reactions measured by DSC with that calculated from the Total Segregation Model confirming the model fits well. This comparison confirms the nature of TGDDM/44DDS/PES prepolymer follows kinetic control in the continuous reactor leading to predictable levels of conversion which is significant for controlling chain-extension reactions and prepolymer viscosities in continuous reactors.

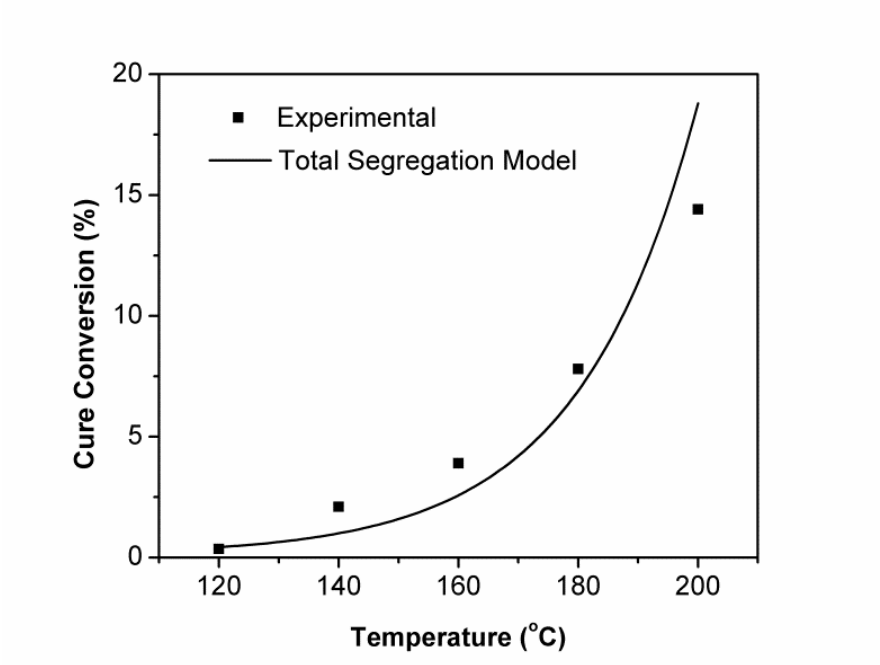

Figure 10. Comparison of simulation vs. experimental in continuous reactor

Phase separated morphology

Further validation for comparison of continuous reactor prepolymers with batch reactor prepolymers was assessed with cured polymer morphologies. In particular, we were interested to observe the reaction induced phase separation behavior of PES within the epoxy networks upon cure. TGDDM/44DDS/PES prepolymers from batch and continuous reaction processes were fully cured and their phase morphologies quantified by AFM using nanomechanical mapping (Figure 11). Both polymers displayed similar domain behaviors in the size-scale range of tens of nanometers of PES phase-separated within the cured network morphologies. The dark domains observed in the DMT modulus image Figure 11 (a) and (b) correspond to the lower modulus PES phases for the batch and continuous reactor polymers, respectively. The brighter features in each

image are associated with the higher modulus epoxy phases. Both cured polymers are similar in phase separated morphology and typical for what we expect to observe for these polymers.

Utilization of imaging software provides an ability to analyze the distribution of size domains and provide a quantitative comparison between samples. A threshold of image color was defined to distinguish between the dark and bright phases shown in Figure 11 (c) and (d) for the batch and continuous reactor polymers, respectively. Again, the general patterns that we observed using this technique suggest similarities in the size and distribution behavior of PES phase separated within the cured TGDDM/44DDS epoxy networks prepared by batch and continuous reaction.

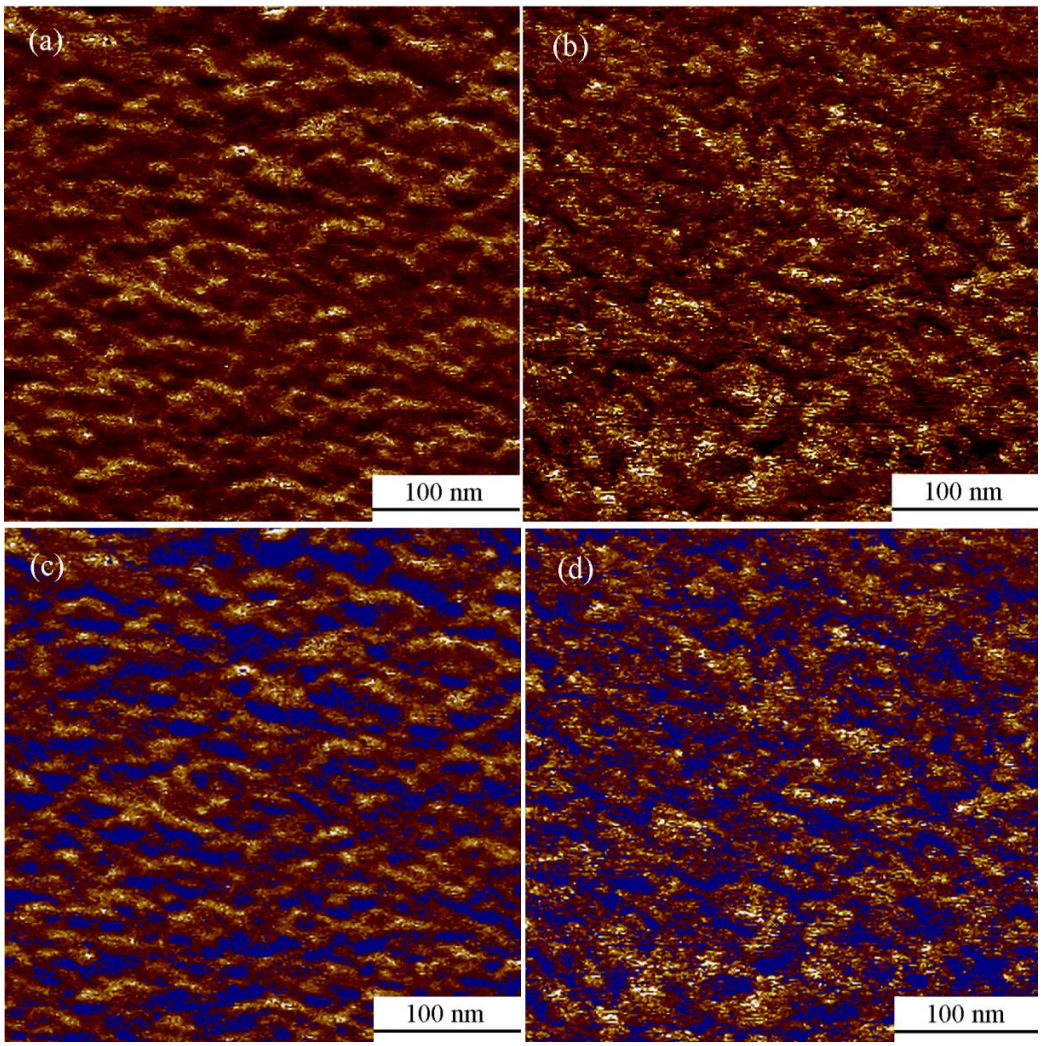

Figure 11. AFM-DMT of cured TGDDM/44DDS/PES systems: (a) batch reaction (b) continuous reaction (c) batch imaging (d) continuous imaging

The calculated histograms of PES domains were shown in Figure 12(a) and (b). Similarities were observed for the average PES domain size diameters calculated at 6.85 nm and 6.12 nm for cured samples prepared by batch and continuous reaction, respectively. Although the average domain size for the continuous reactor material is slightly smaller as evidenced by the calculated average diameter and histogram count observed in Figure 12, these domain size variances are well-within expected ranges for the example TGDDM/44DDS/PES formulations. We conclude the

cured morphologies of TGDDM/44DDS/PES polymers from the batch and continuous reactors are the same.

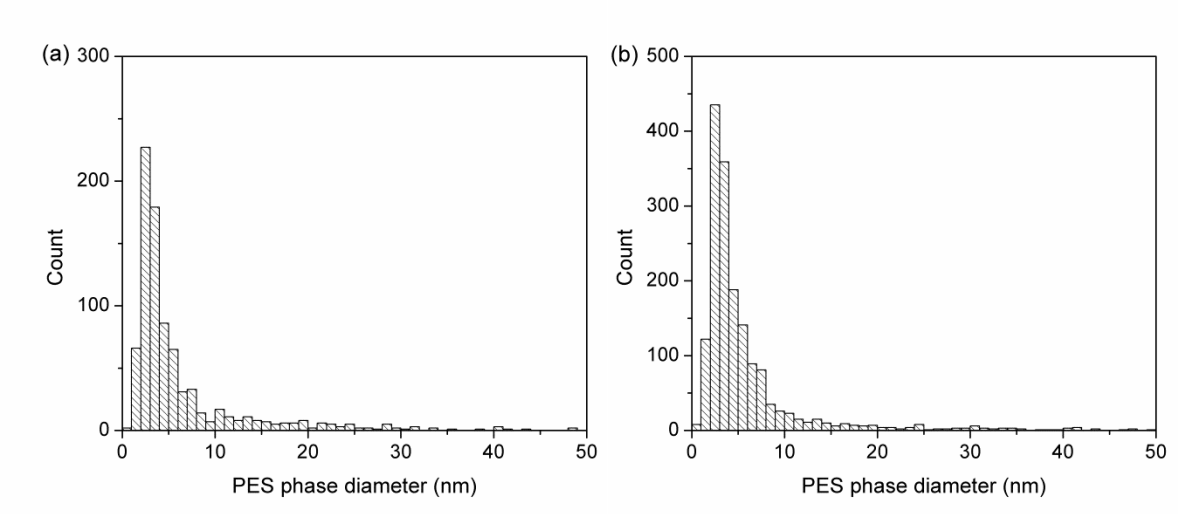

Figure 12. PES phase diameter histograms of (a) batch reaction and (b) continuous reaction

Mechanical properties

Mechanical properties of cured TGDDM/44DDS/PES polymers produced by batch and continuous reactors were measured to compare tensile strength, tensile modulus, tensile elongation, and fracture toughness shown in Table 3. In all cases, mechanical properties are statistically similar for both cured polymers and well-within in property values and standard deviations for these glassy polymer networks.

Table 3. Mechanical properties of cured TGDDM/44DDS/PES system

Samples	Tensile Modulus (MPa)	Tensile Stress (MPa)	Elongation at Break (%)	K_{IC} (MPa $m^{1/2}$)
Batch Reactor	3040 ± 1 %	60.9 ± 5 %	4.3 ± 4 %	0.709 ± 10 %
Continuous Reactor	3032 ± 6 %	65.4 ± 10 %	5.1 ± 12 %	0.757 ± 8 %

2. Aerospace Composite Nano-Matrix Continuous Prepolymer Reactor Developed

Our high-shear aerospace prepolymer matrix preparation techniques described above provided a new and novel method for preparing nanoparticle modified epoxy prepolymers for advanced aerospace materials development. The advancement of epoxy chain extension or conversion was controlled by reaction chemistry, process designs and processing conditions in order to achieve targeted viscosities with tack optimized for prepreg filming applications. The biggest advantages to this continuous reactor design, when compared to the batch process it replaced, was the mitigation of batch-to-batch variation, favorable performance measures relating to processing rate, namely the reduction of space-time and augmentation of space-velocity for the system, and the abatement of conditions where large volumes of reactive materials are involved in which safety concerns arise. Our intention through the present research was to combine our successful strategies for advancing epoxy chemistries with our approach to achieve high levels of nanotube dispersion using a continuous reactor. We believe MWCNT dispersion and stabilization in epoxy matrix can be drastically improved via a continuous reaction process, as opposed to conventional methods, owing to the unique advantage of

controlling prepolymer matrix viscosity. To the best of our knowledge, a solvent free and single-step approach to formulate epoxy resin, curative, and nano-reinforcement has not been reported. The development of an economical process for producing large quantities of epoxy matrix prepolymers modified with carbon nanotubes has certain value in the aerospace and other composites communities. It was the goal in this portion of our research to highlight the dispersive capabilities of the high-shear continuous reactor and the benefits to disperse and stabilize nanoparticles. Using the reactor setup, as described in the present work, *carbon nanotubes have been successfully dispersed at concentrations from 0.02% to 26.0% by weight into TGDDM based aerospace composite prepolymers at continuous reaction rates exceeding 30 LBS/h.*

Over the past decade the mechanical, electrical and thermal properties of carbon nanotubes have spurred intensive investigations aimed at developing nanostructured composites. Multiwall carbon nanotubes (MWCNT) have the potential to impart desirable properties of epoxies including electrical and thermal conductivity and mechanical performance. However, the experimentally observed properties depend heavily on the dispersion state of the nanotubes. The strong tendency of MWCNT to agglomerate in epoxy matrices often lead to cured networks with diminished material properties. Increased capabilities and efficiencies in the production of specifically MWCNT have made them more conceivable as electrical and thermal modifiers in industrial applications for high performance composite materials.

High quality of MWCNT dispersion is difficult to obtain for several reasons. First, there is a large amount of energy required to overcome the van der Waals interactions between neighboring tubes. This causes them to stick together in primary agglomerates and recombine into secondary agglomerates after a dispersion event. Second, determination of nanotube quality

is not straight forward and is not always reflected in the comparison of properties listed by manufactures. Differences in nanotube properties make direct comparison of literature studies difficult and can further complicate the already exhaustive process of exceptional nanotube dispersion. Lastly, the quantification of dispersion state is difficult. Despite decades of research, there still does not exist a single accepted method of dispersion quantification that takes into account the continuum of length-scales relevant to fully describe a dispersed state for nanofillers like MWCNT. Despite these challenges, several approaches have been developed to promote MWCNT dispersion in polymer matrices. These approaches include mixing techniques such as sonication[, high shear mechanical mixing, and calendaring,[as well as chemical techniques such as surface functionalization and use of dispersive surfactants. Unfortunately these techniques are often limited to small quantities because of the impractical nature of operation at larger volumes. This is due to the excessive amount of heat generated by the high localized shear and inefficiency associated with these methods.

It is well understood that an increase in shear, applied to a system, translates as an increase in dispersion state. This is due to the relationship between shear force (τ) matrix viscosity (μ), boundary velocity (u), and distance from shear boundary (y) is presented in Equation 4. Shear force scales with viscosity and, thus, it is expected that dispersion states would increase with increasing polymer viscosity. Therefore, it is desirable to develop a dispersion method that is not only capable of handling, but makes use of, the high shear forces that arise from high viscosity matrices. Methods of dispersion such as ultrasonication, mechanical mixing, and calendaring require low viscosity media which limit their use, not only in the shear forces they invoke on agglomerates, but also, in the ability to curb re-agglomeration of nanotubes in the highly dynamic and mobile media environment.

$$\tau(y) \propto \mu\frac{\partial u}{\partial y} \quad (4)$$

High-shear continuous reactors, where the reactor is a twin screw extrusion (TSE), offer the capability to handle high viscosity materials and has acquired great interest for research as an environmentally-favorable and economic method for industrial scale manufacturing. More specifically, fully intermeshing co-rotating twin screw extruders offer the highest level of mixing, dispersion, and shear control, making them the primary technology used as continuous chemical reactors. Typically this method is associated with dispersing nanoparticles within high molecular weight linear thermoplastic polymers. In this process, during melt mixing, the applied shear strength is directly tied to the agglomerate size reduction. Several studies reported greater dispersion was achieved by using high melt viscosity matrices thereby maximizing the shear environment and shear states applied. However, extrusion processes are limited in their ability to disperse nanoparticles into epoxy matrices, since epoxies are generally used or processed in a low viscosity state and therefore result in unfavorable shear environments within the reactor barrel.

Engineered nanocomposite prepolymers of TGDDM/MWCNT were prepared using a continuous reaction method which was accomplished using a Coperion ZSK 26 mm co-rotating intermeshing twin-screw extruder (L/D = 40). The continuous reactor was modular and specifically designed for the epoxy-amine cure reaction and MWCNT dispersion in a single step process. As illustrated in Figure 13, the reactor and screw profile consists of a liquid feed zone (Zone 1), a solid feed zone (Zone 2), ten electrically heated and liquid cooled zones (Zone 1-10), and an additional zone to control the thermal profile of the melt pump. The hot zones (Zone 1 to 6) were kept at the same elevated temperature between 160 °C and 200 °C which previous work

has shown to be an ideal temperature range for the complete dissolution of 44DDS in TGDDM and the advancement TGDDM prepolymer viscosity without concerns of gelation in the continuous reactor.[32] The cold zones (Zone 7 to 10) also had a static temperature profile that varied from 40 °C to 100 °C. Screw design was configured to balance shear mixing and residence time, which was found to be between one and two minutes, with a combination of various conveying, kneading, gear and reverse elements. The screw design was optimized to the incorporate two kneading block sections to provide adequate shear mixing. Gear and reverse elements were incorporated in Zone 8 to optimize the residence time, generate back-pressure and enhance MWCNT dispersive and distributive mixing. A vacuum pump was attached at Zone 9 and was used to remove volatiles, between the melt seals formed at the reverse element in Zone 7 and the melt pump, to reduce trapped air that would otherwise form bubbles during cure. The benefits of this two-step temperature profile include the ability to control epoxy prepolymer properties such as molecular weight and tack, all the while maximizing MWNCT dispersion and stabilization through to the final cured composite.

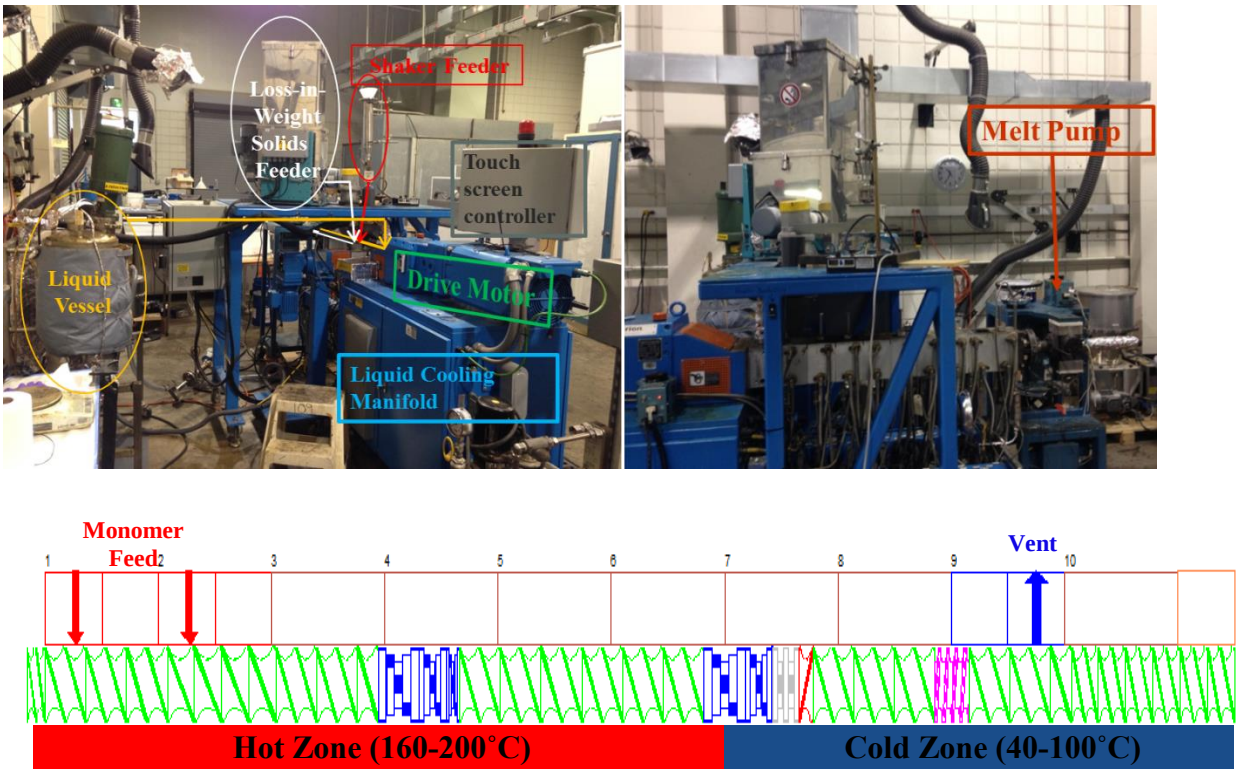

Figure 13. Reactor and screw configuration nanocomposite prepolymer preparation.

For a typical continuous reaction, TGDDM was pre-heated to 80 °C in a 50 L batch reactor and delivered into the continuous reactor through a liquid feed port in Zone 1 at a rate of 47.7 g/min. 44DDS was charged into a gravimetric solids feeder to deliver a rate of 28.0 g/min which gave 1:1 stoichiometric equivalents of epoxy to active amine hydrogen. MWCNT was fed by a laboratory vibratory feeder capable of consistent feeding rates as low as 0.01 g/min. Both 44DDS and MWCNT were added through a side stuffer at Zone 2. Aliquots of extrudate material were collected just beyond the melt pump and quenched in a freezer for characterization. Table 4 describes the nomenclature, compositions and processing conditions employed within this work for TGDDM/MWCNT prepolymers.

Table 4. TGDDM/MWCNT prepolymers nomenclature, compositions and processing conditions

Sample No.	MWCNT content (wt %)	Hot zone temperature (°C)	Cold zone temperature (°C)	Screw speed (rpm)
1	1.0	160	60	600
2	1.0	180	60	600
3	1.0	200	60	600
4	1.0	180	40	600
5	1.0	180	80	600
6	1.0	180	100	600
7	1.0	180	60	200
8	1.0	180	60	400
9	1.0	180	60	800

DSC was performed using a TA Instruments DSC Q200 to study the glass transition temperature (T_g) and cure conversion in the epoxy prepolymers at various processing conditions. A heating rate of 5 °C min^{-1} was employed in the temperature range of -20 °C to 300 °C under nitrogen. The T_g for the prepolymers was reported as the peak maximum within the heat capacity trace. Residual curing enthalpy (ΔH_{res}) was used as an indicator for the degree of cure for the epoxy prepolymers and calculated from the exotherm peak area in the DSC thermogram.

Rheological analysis was conducted on an ATS Rheosystems rheometer with disposable 25 mm parallel plates to measure the complex viscosity (η^*) of epoxy prepolymers and their development during isothermal cure. Experiments were performed within the linear elastic regime at a strain of five percent and a frequency of 1 Hz.

An Olympus GX51 metallurgical microscope with a reflection light source was used to examine the MWCNT dispersed states and their stability in the TGDDM prepolymers. Samples were prepared by sandwiching a thin layer of sample between two pieces of cover glass using one layer of 0.02 mm thick Teflon film to act as a spacer to maintain a uniform sample thickness. The dispersion states of the nanocomposite prepolymers were quantified using an Olympus Stream Image Analysis software package. Dispersion index, *D* which reflects the normalized agglomeration area was calculated according to Eq.5:

$$D = \left(1 - f\frac{A_{CNT}/A_0}{\emptyset_{vol}}\right) \times 100\% \quad (5)$$

The area occupied by MWCNT agglomerates A_{CNT} and the total investigated area A_o were obtained from image analysis in which agglomerates with diameters smaller than 1 μm were neglected. $\emptyset_{vol}$ is a term to describe the nanotube volume fraction and *f* is a factor related to the density of CNT agglomerates and was estimated to be 0.25. According to Eq.2, a *D* value of 100 % corresponds to a perfect micro-scaled dispersion in which all the nanotubes are contained within agglomerates less than 1 μm in diameter within the sample. A decreasing dispersion state is reflected in a decreasing *D* value. Average *D* values reported in the current study were determined from optical images taken from five representative locations within each sample.

A Zeiss EM900 transmission electron microscope (TEM) was used to probe the carbon nanotube dispersion at the sub-micron scale with an accelerating voltage of 50 kV. Samples were cut into ultrathin (~100 nm), trapezoidal shaped sections with a Porter-Blum MT-2B microtome using a diamond knife at room temperature. Sections were collected on a 200 mesh copper TEM grid and imaged without staining.

Several key processing parameters are discussed to highlight crucial control variables and benchmark properties of TGDDM/MWCNT prepolymers produced via the continuous reactor. The hot zone was designed to partially cure, or B-stage, the matrix using the barrel temperature to control the extent of reaction between the epoxide resin and amine curative. This aim was demonstrated through the preparation of TGDDM/MWCNT prepolymers with varying hot zone temperatures (160 °C, 180 °C, and 200 °C) with a constant cold zone temperature of 60 °C and their properties were examined by DSC. A threshold condition of 200 °C was used as the maximum hot zone temperature to avoid system gelation and prevent runaway crosslinking within the barrel of the extruder. This temperature was determined experimentally through isothermal cures of the TGDDM 44DDS matrix system on a parallel plate rheometer to track the time to gelation within the viscoelastic regime. Comparison of this time-to-gel with the known residence time of the continuous reactor afforded the determination of this celling temperature with a factor of safety and confidence built in.

Figure 14 shows the DSC curves for the TGDDM/MWCNT prepolymers during the heating stage from 0 °C to 300 °C. As expected, all thermograms follow a similar motif, but with T_g and residual heat of cure (ΔH_{res}) which correspond to the extent of B-staging. These values are tabulated in Table 5. The T_g increased from 5.1 °C for the 160 °C sample to 8.0 °C for the 200 °C sample while ΔH_{res} reduced from 608.7 J/g to 582.8 J/g, suggesting that the temperature of the hot zone did indeed advance the conversion of the prepolymers significantly. In the continuous reactor, the cure reaction took place immediately after TGDDM and 44DDS mixed in the hot zone. The cure reaction is kinetic-controlled prior to reaching its gel point, with the cure rate being sensitive to cure temperature in an Arrhenius relationship. Thus, increasing the hot zone temperature increases the reaction cure rate, consequently leading to higher glass transition

temperatures and cure conversion. An inflated polymer T_g yields an additional increase in viscosity within the cold zone portion of the reactor barrel.

Table 5. Properties of TGDDM/MWCNT prepolymers at different hot zone temperatures.

Sample No.	Hot zone temperature (°C)	T_g (°C)	ΔH_{res} (J/g)	η (Pa·s)*
1	160	5.1	608.7	1.0
2	180	6.5	597.3	3.7
3	200	8.8	582.8	5.5

** Prepolymer viscosities were measured at 80 °C.*

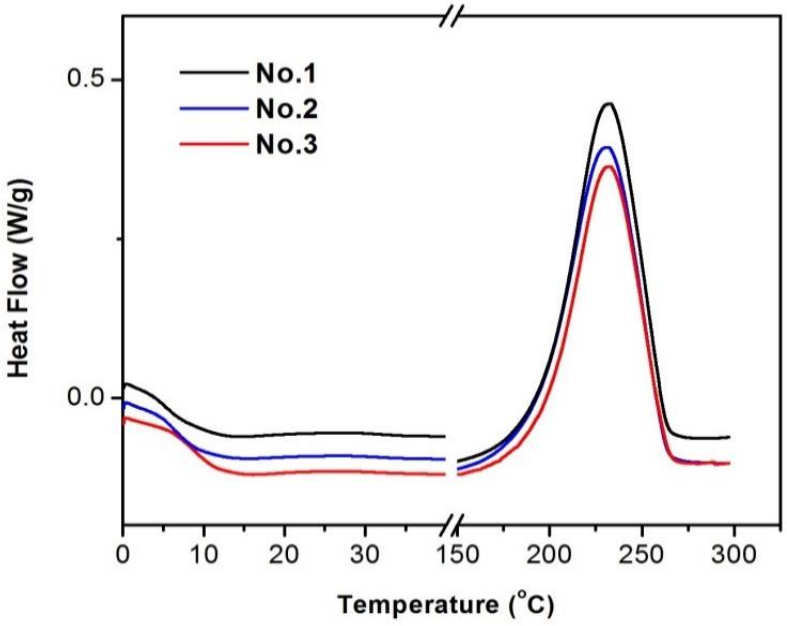

Figure 14. DSC exotherms for prepolymers prepared at different hot zone temperatures

This increase in prepolymer viscosity is thought to serve two purposes; first it increases the shear environment the nanotube agglomerates experience within the cold zone of the reactor. Second, it acts to better stabilize, or lock in, the nanotube dispersion state mitigating secondary agglomeration through an increased rheological state. The ability to tailor the viscosity of epoxy prepolymers through the control of hot zone conditions confirms the feasibility of using the hot zone to control epoxy prepolymer properties. This is particularly useful for maintaining processability and tack for use in aerospace prepreg filming applications, which is essential for high T_g epoxies.

The agglomerate distributions of nanotubes in the TGDDM based prepolymers, prepared at three hot zone temperatures were investigated. Very similar dispersion states were observed for all three conditions. To provide a statistical comparison, their dispersion indices were calculated using Eq.5. *D* value of 97.9%, 98.5%, and 98.3% were obtained for 160 °C, 180 °C, and 200 °C samples respectively. Since their difference in dispersion index fell within the statistical error ranges, the data suggests that changing the hot zone temperature from 160 °C to 200 °C has little influence on MWCNT dispersion, at least prior to cure. To reiterate, it is the purpose of the hot zone to control the extent of the epoxy chain extension reaction, which is hypothesized to have an effect on the extent of stabilization of the dispersed state during cure.

Twin screw high shear continuous reactors are not traditionally designed for low viscous epoxy prepolymers since the shear force imposed on the resin between screw flights and the barrel deteriorates rapidly as the viscosity decreases. When this occurs the particle mixing and dispersing event becomes inefficient. While the purpose of applying the hot zones is to advance the resin cure conversion and viscosity helps to mitigate this issue, the cold zones are designed to further enhance the nanotubes dispersion within the prepolymer matrix. A reduction in cold zone

barrel temperature significantly increases the processing viscosity of epoxy resin which aids the carbon nanotube dispersion by augmenting the shear environment.

Samples were prepared at four cold zone temperatures (40 °C, 60 °C, 80 °C, and 100 °C) using a constant hot zone temperature of 180 °C and their dispersion states were examined via optical microscopy. Figure 14 illustrates the MWCNT dispersion states developed in these epoxy prepolymers at the described processing conditions. Comparison of the pristine MWCNT, shown in Figure 2, to the dispersion obtained through the continuous processing shows a distinct size reduction from around 500 μm to 10 μm that was observed for all cold zone processing conditions, suggesting the excellent dispersive mixing ability of the continuous reactor. Samples prepared at the lowest cold zone temperatures of 40 °C and 60 °C (No.4 and No.2) showed MWCNT agglomerates that were evenly distributed in the prepolymer matrices. Few isolated bundles larger than 1 μm were observed, characteristic of the high dispersion indices observed for these samples. The increase of cold zone temperature up to 100 °C, lead to increases in both the number and size of MWCNT agglomerates. For example, sample No.6, with cold zone temperature of 100 °C, was dominated by the largest agglomerates with diameters of ~20 μm.

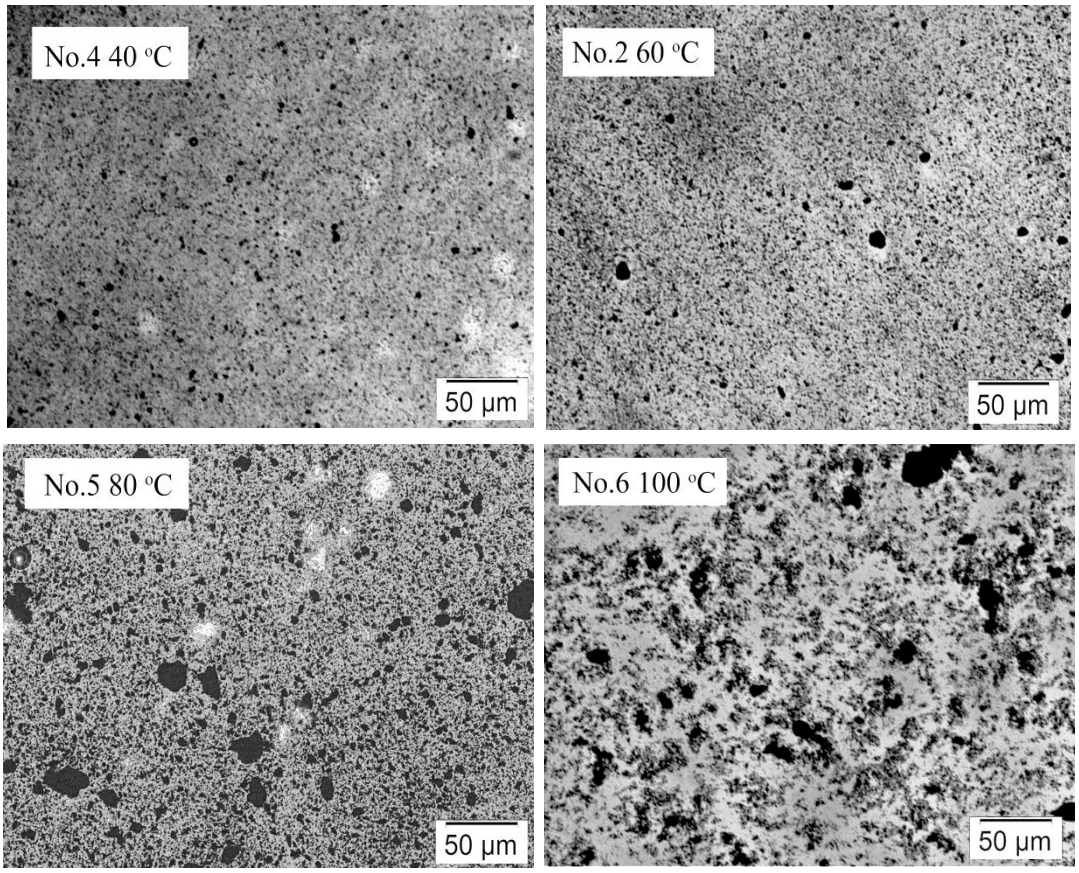

Figure 14. Optical images showing effect cold zone temperature on dispersion.

The effect of nanotube dispersion at varying cold zone temperatures was quantified by the designation of dispersion indices which are tabulated in Table 3 and clearly reflect the qualitative trends observed in Figure 14. Samples prepared at 40 °C show dispersion index values eclipsing 99%, suggesting nearly homogenous micro-scale dispersion. The value of *D* decreased from 99.2 % to 84.5 % as the cold zone temperature increased from 40 °C to 100 °C. This reflects the reduction in shear environment with respect to matrix viscosity controlled by cold zone barrel temperature. This shear environment is effective for improving nanotube dispersion in epoxy prepolymer matrices.

Although, the shear stress applied on the carbon nanotubes is primarily responsible for the MWCNT agglomerate size reduction, the direct measurement or calculation of shear stresses within the barrel of the TSE is not straight forward. This is due to the dynamic and reactive nature of the epoxy resin, progression of reaction, and the complexity of the screw profile. We can only speculate on these shear states based on the post-processing viscosities of the prepolymers, which are proportional to the shear stress at a constant screw speed. Table 3 shows the viscosity of each of the nanocomposite samples determined at the cold zone temperature in which they were processed. Decreasing the cold zone temperature from 100 °C to 40 °C increased the viscosity three orders of magnitude from 2.7 E+0 Pa·s to 1.3 E+3 Pa·s which would suggest that the shear environment invoked on the tubes was about three decades higher in the 40 °C samples owing to the increased breakup of the nanotube bundles and improved dispersion observed at the micron scale.

Table 6. Dispersion indices and viscosities of different cold zone temperatures

Sample No.	Cold zone temperature (°C)	D (%)	η (Pa·s)*
2	40	99.2	1.3 E+3
4	60	98.5	1.2 E+2
5	80	94.6	0.8 E+1
6	100	84.5	2.7 E+0

**Processing viscosities were measured at the corresponding cold zone temperature aliquots*

Samples with the best and worst nanotube dispersion state, No.4 and No.6 respectively, were imaged via TEM to better understand the multi-scale dispersion state, and to highlight the influence of cold zone temperature, within these materials. Figure 15 illustrates the sub-micron dispersion for the material prepared at 100 °C. Large unreinforced areas of matrix were observed surrounding localized areas of high nanotube density. Samples prepared at 40 °C showed the highest level of dispersion at the micro-scale and presented a more uniform dispersion at the sub-micron scale and exhibit the smallest diameter agglomerates. The significant improvement in carbon nanotube dispersion at both length-scales demonstrates the importance of cold zone temperature during continuous reaction.

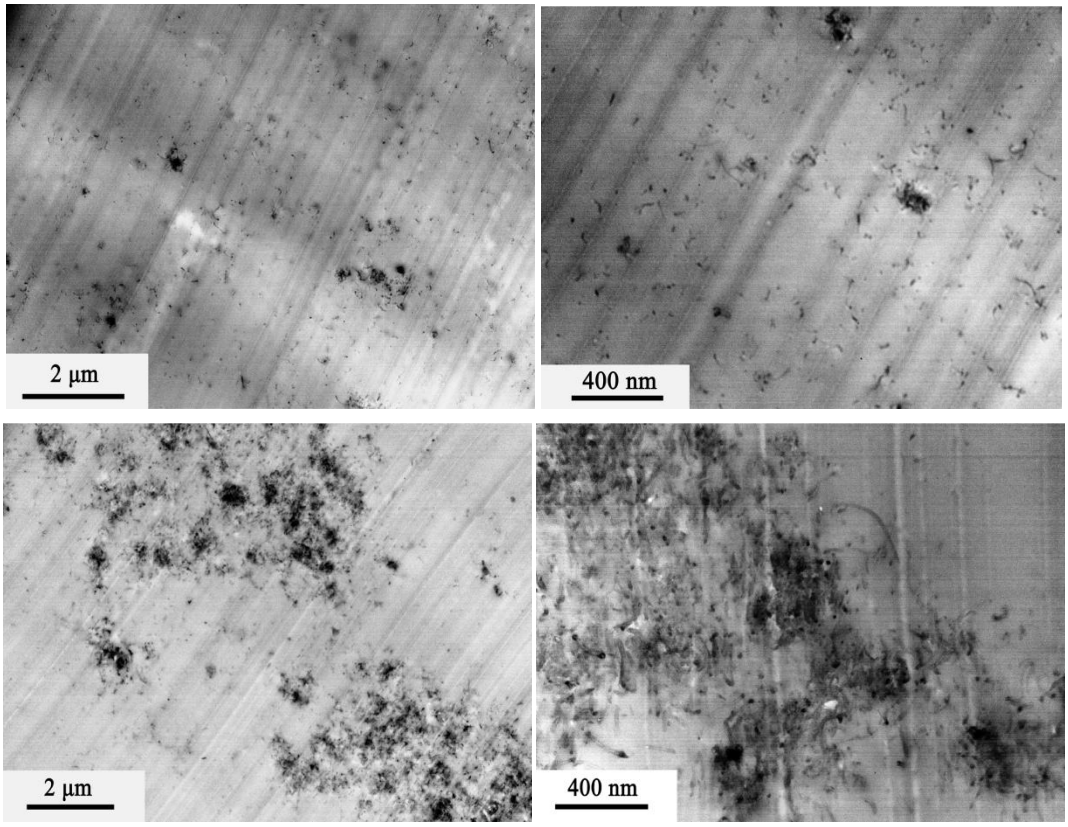

Figure 15. TEM images of samples prepared from different cold zone temperatures. Top: Sample No.2 processed at 40 °C; Bottom: Sample No.6 at 100 °C

At the centers of many of the most densely packed agglomerates, we observe small crystalline impurities that we believe to be residual catalyst left over from the synthesis of the tubes. It is possible that these impurities may be acting as nucleation points for agglomeration resulting in an inferior dispersed state. This result suggests that impurities are critical to the agglomeration state within these materials.

Unlike thermoplastic polymers, dispersion of MWCNT in epoxy matrices is more complicated as epoxy prepolymers require curing before practical use. When temperature is raised above ambient conditions the viscosity of the resin matrix drops significantly, which affect MWCNT dispersion stability and favors re-agglomeration. Good nanotube dispersion is often retained in the uncured epoxies but reagglomeration is observed in the final cured composites. In this study, however, no apparent change in carbon nanotube agglomerate size was observed at the micron scale comparing prepolymers and cured specimens. This was accomplished by progressing cure beyond the point of gel isothermally at 80 °C over the course of two days and then post curing the samples at 200 °C to further drive conversion. This cure prescription was chosen specifically to minimize the drop in matrix viscosity that would otherwise accelerate nanotube agglomeration in high temperature cure cycles. In this way we could observe dispersion at the sub-micron length-scale using TEM in fully cured nanocomposite materials. It is important to note that the success of this low temperature cure cycle on leaving dispersion state intact is conspicuously bound to the partial curing of epoxies within the hot zone region of the reactor. This finding brings a new approach to the stabilization of carbon nanotube dispersions and subsequent restrictions of re-agglomeration through the partial curing of the matrix.

Continuous reactor screw speeds were varied to further demonstrate the continuous reactor capabilities in nanoparticle dispersion. The nano-scale dispersion states of MWCNT samples prepared at 200 rpm, 400 rpm, 600 rpm and 800 rpm are shown in Figure 16 with their dispersion indices plotted as a function of screw speed being presented in Figure 17. The 200 rpm sample showed the lowest level of dispersion among all the samples with a *D* value of 89.8 %. Increasing TSE screw speed led to an improved dispersion state peaking at 600 rpm. Only a small degree of change was observed between 600 rpm and 800 rpm, indicating that there may be a limit to the influence of screw speed on the ability to promote additional dispersion of MWCNT in epoxy matrices. Higher screw speed generates higher shear stress during continuous reaction process, facilitating MWCNT agglomerates breakup and enhancing their dispersion in epoxy prepolymer matrices. However, residence times are reduced with increasing screw speed, which leads to the diminishing returns observed. Therefore, the counteracting balance between shear stress and residence time on MWCNT dispersion is observed at around 600 rpm in this study.

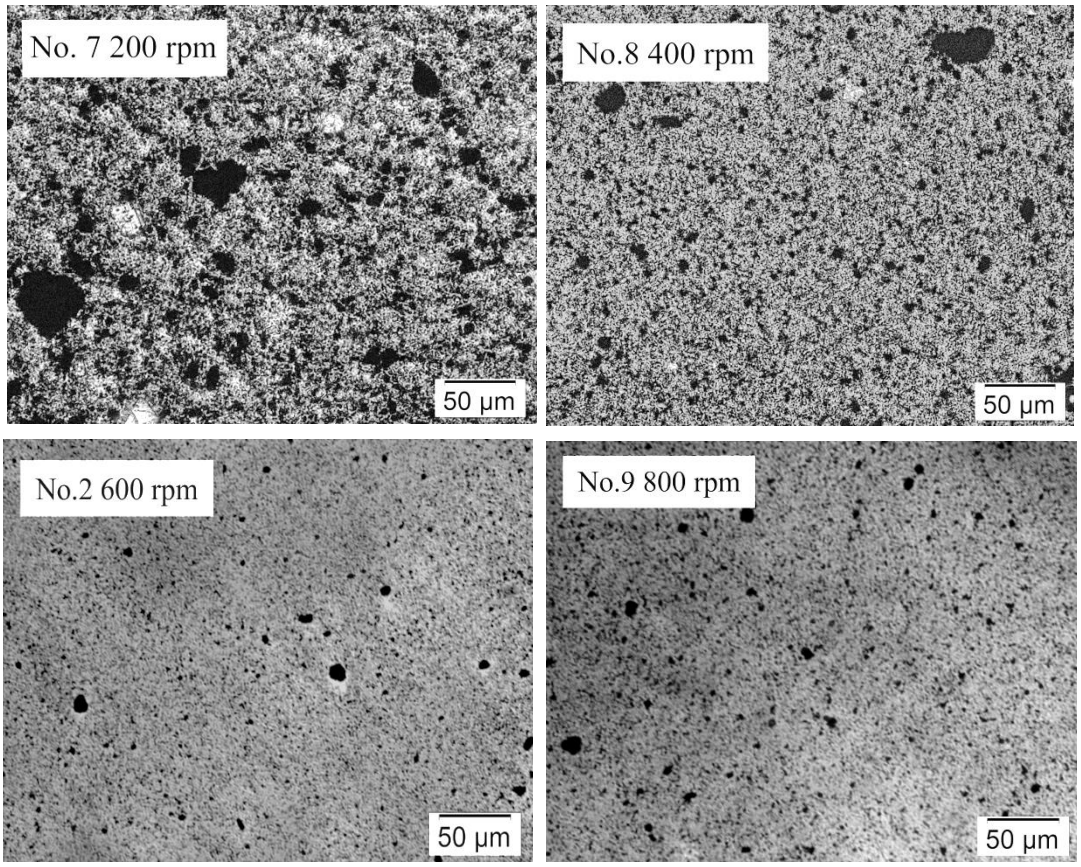

Figure 16. Optical images of TGDDM/MWCNT prepolymers at different screw speeds

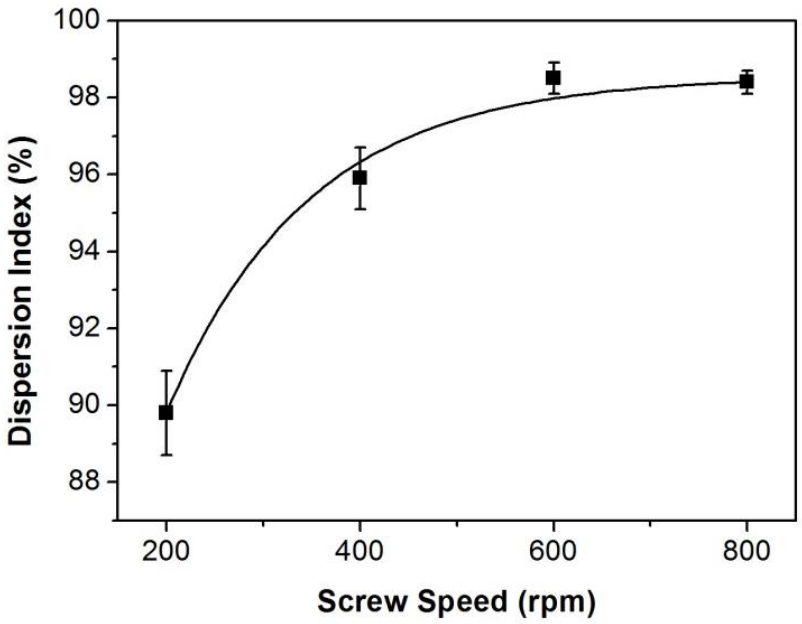

Figure 17. Dispersion indices of TGDDM/MWCNT prepolymers versus screw speed.

We investigated several grades of MWCNT in this research. Baytubes from Bayer Material Science were used as the basis of our preliminary work due to their low cost and availability. As mentioned in the prior section, we observed a high degree of impurities which are expected for the low-cost MWCNTs. The dispersion of Baytubes allowed for the determination of reactor processing conditions that lend themselves most favorable to high quality dispersion of MWCNT in epoxy prepolymers. To better demonstrate the dispersive capacity of this method and better investigate the effect of impurities on the dispersion of the system, the authors would present to you the result of our highest performing processing conditions on dispersing high quality MWCNT where the effect of impurities could be compared directly. This was accomplished through the dispersion of two new types of MWCNT namely SMW200 and SMW210, which are produced by SouthWest Nanotechnologies and are identical

in composition with the exception that the SMW200 tubes are a higher purified version of the 210 type absent of most residual catalyst and other impurities. Nanocomposites of these higher purity tubes were prepared using the optimized conditions determined above, namely hot and cold zone temperatures of 180 °C and 60 °C respectively and a screw speed of 600 rpm. Figure 18 shows TEM images of 2.0% wt/wt loaded composites demonstrating the sub-micron dispersion states realized in the presence and absence of molecular level impurities. The residual impurities, observed as dark black squared off particles, in the unpurified samples again appear to be the nucleus of all of the largest nanotube agglomerates. In contrast, neither the impurities nor the largest agglomerates were observed in the samples made with the purified nanotubes and therefore result in the highest dispersed state.

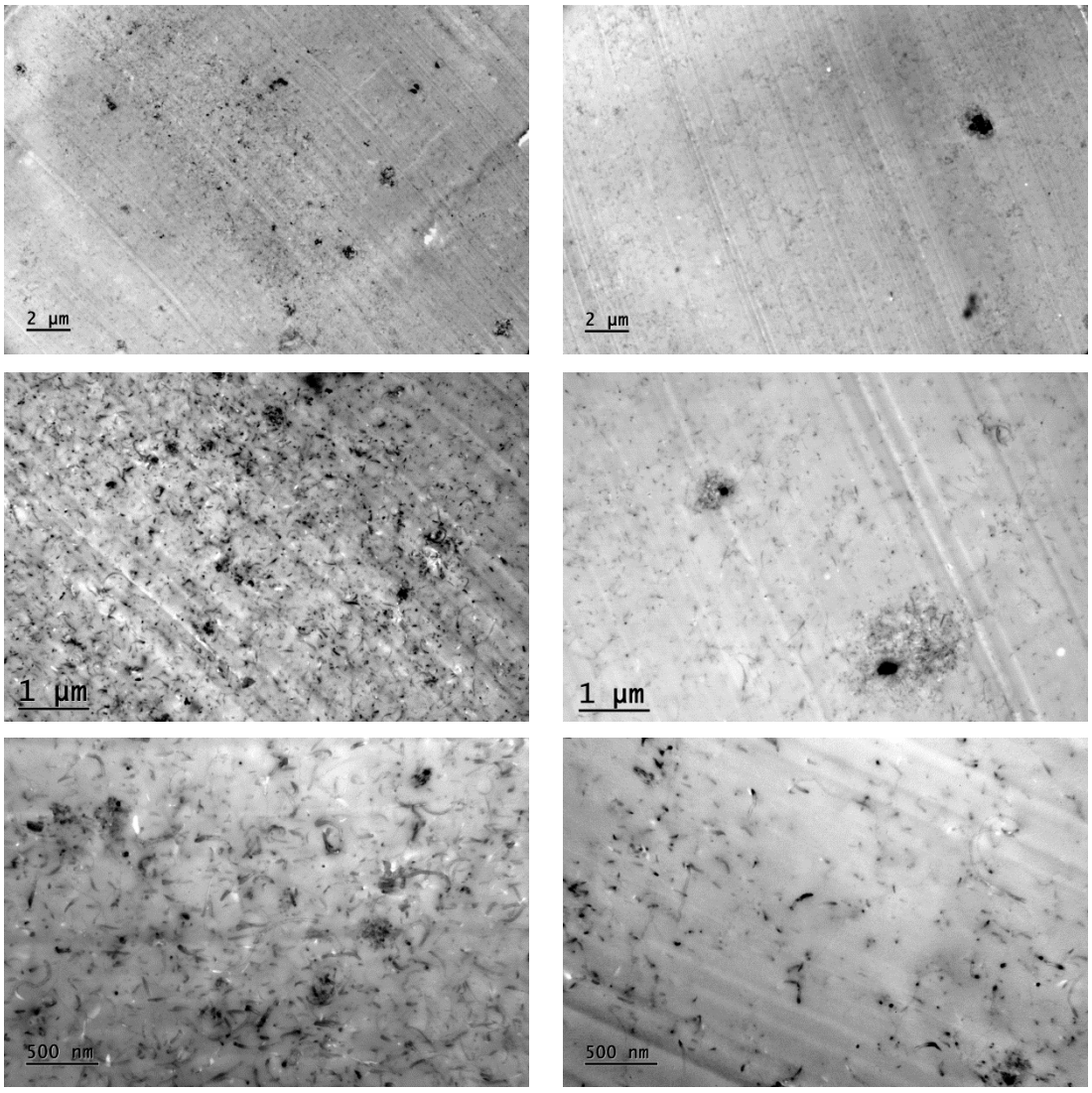

Figure 18. TEM images of composites containing 2.0% wt/wt SMW200 (purified - left column) and SMW210 (unpurified - right column).

Bulk material conductivity was used as an indirect metric to quantify dispersion state. Figure 19 illustrates the results of this comparison in which premiminary conductivity of the nanocomposites formulated with SouthWest tubes are consistently one decade higher when compared above percolation threshold. We attribute this increase in bulk conductivity to the improved dispersion state brought on by the superior tube quality associated with the SouthWest

tubes. For comparison sake, at 5.0% wt/wt loading the bulk conductivity of the Baytube sample was 0.06 S/cm compared to 0.35 S/cm for both the SMW200 and 210 samples. Although higher concentrations of tubes have not yet been investigated for the SouthWest tubes, the conductivity for Baytubes at 26% wt/wt has been demonstrated as high as 0.84 S/cm and, providing the trend in comparative conductivities continues, it would be reasonable to expect SouthWest composites to approach the 5-10 S/cm range, which would be an exceptional result for this class of material.

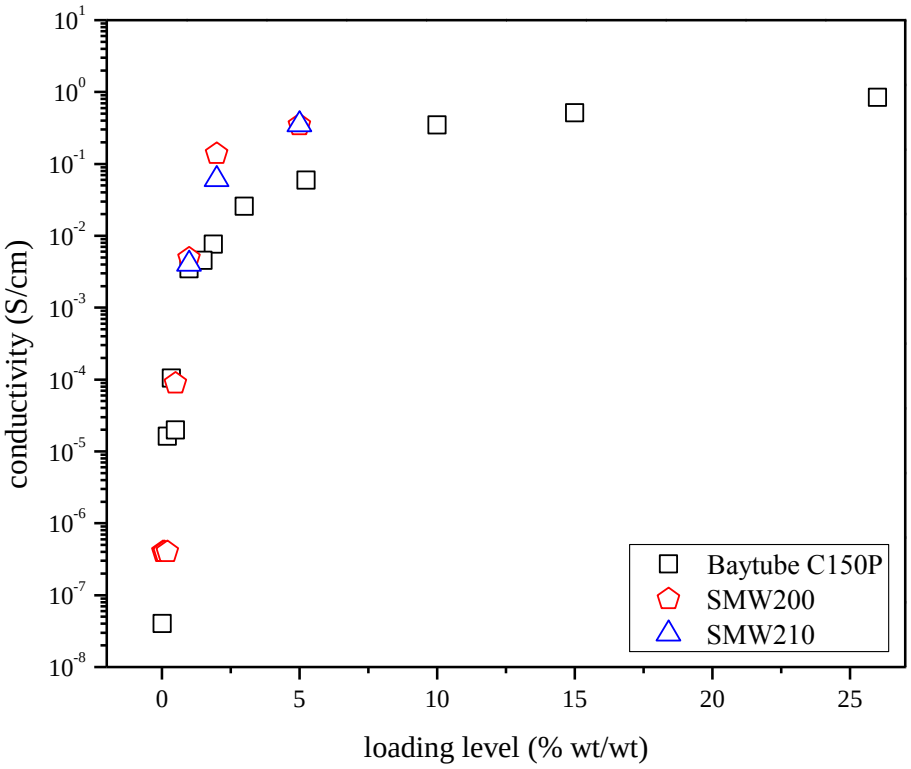

Figure 19. Four-point probe bulk conductivity measurements for cured MWCNT composites.

Impact of Results

MWCNT nanocomposite aerospace prepolymers were successfully prepared in a one-step high volume process through the development of a new preparation approach based upon a high-shear continuous reaction method. The continuous reactor based upon two principle advancements in process engineering.

1. Chain extension prepolymer reactions including curative dissolution, toughener dissolution and controlled chain-extension reactions in the continuous reactor high temperature "hot-zone" to advance conversion, rheology and tack.
2. Simultaneous MWCNT dispersion and stabilization in the continuous reactor low temperature "cold-zone" leading to an increased viscosity and stabilization of MWCNTs within rheological regimes which inhibit re-agglomeration to aid in post processing stabilization of dispersion state through final cure.

The significance of this work is the demonstration of a new method to prepare fully dispersed MWCNT aerospace prepolymers, from reactants to finished products in under 90 seconds reaction time (Figure 19). This reactor technology provides a new pathway for preparing a broad array of aerospace composite matrix prepolymers through simultaneous reaction, mixing and blending of a broad array of co-reactants, modifiers, and nanoparticles. This new approach is a significant advancement in nanoparticle dispersion and stabilization for aerospace composite matrix prepolymers since it is 100% solids, solvent-free, low energy and more environmentally friendly than any other dispersion technology. The continuous reactor is readily scalable and provides benefits of increased production scale, substantial economic favorability, and modular

reactor designs which allow for increased control over prepolymer rheological profiles, low-to-high controlled shear environments and significantly reduced energy consumption.

Figure 19:15% MWCNT epoxy nanocomposite prepolymer (30 LBS/h; 90 sec residence time)

3. Aerospace Composite Nano-Matrix Prepreg Process Developed

Aerospace quality prepreg films were prepared for the MWCNT prepolymers using roll-coating and knife-over-plate doctor blade film. High quality films ranging between 15 to 40 gsm (grams per square meter) loaded between 0.05% to > 20% MWCNT fully dispersed in various aerospace composite epoxy matrix prepolymers were achieved. We have demonstrated the MWCNT nano-films were able to be controlled well-within typical aerospace tolerances and in total we prepared >1000 linear feet of various films in this research. Figure 20 shows the nanocomposite loaded onto a production scale roll coater used to prepare aerospace films for the production of prepreg. The aerospace nanocomposite prepolymers prepared in this research were fully investigated and determined to be produced at appropriate rates. Figure 21 shows a 7”

aerospace nano-film prepared from a knife-over-plate coater which could be used as a carbon fiber impregnation matrix, or used as a "prepreg skin material" applied as an interlaminar layer within aerospace composite structures.

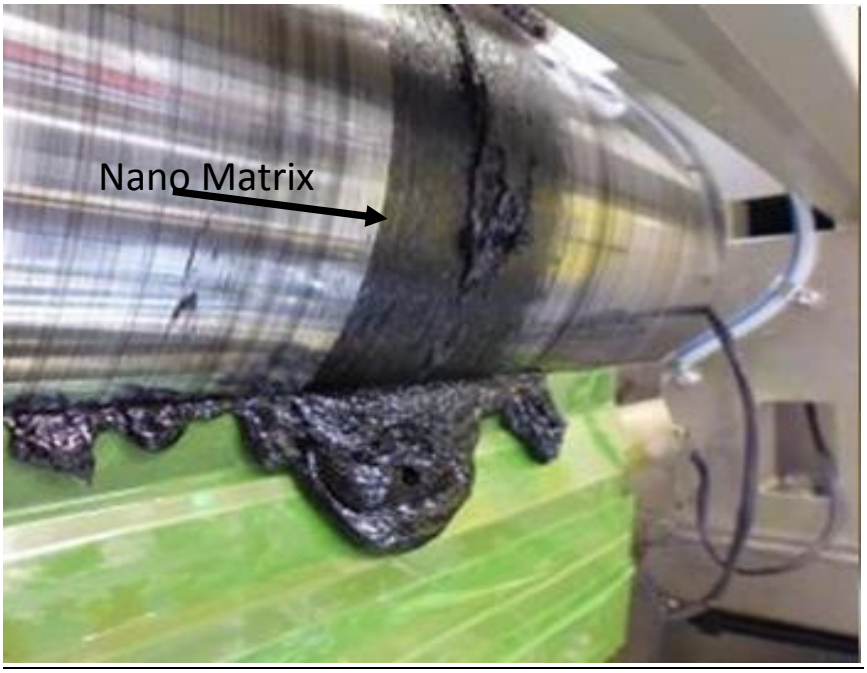

Figure 20: 15.0% MWCNT aerospace epoxy loaded onto an industrial roll coater

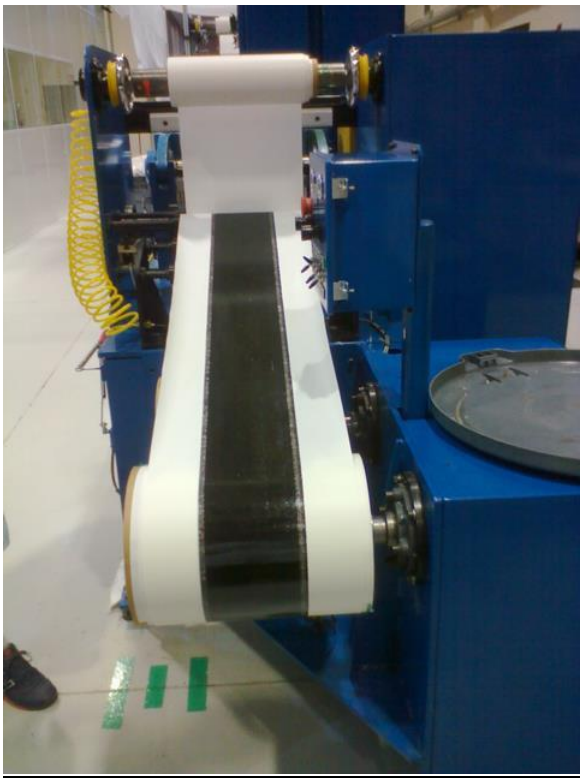

Figure 21: 1.5% MWCNT aerospace film prepared from a knife-over-plate coater

As mentioned above, nano-films have been investigated as impregnation matrices. In this example, the MWCNT matrices of various aerospace chemistries and loading levels are used to fully impregnate carbon fibers during the prepreg preparation process. Figure 22 (left) shows a 12" wide and 10wt% MWCNT nano matrix film being applied onto the surface of dry carbon fiber as an impregnation prepolymer. Figure 22 (right) shows the unidirectional 12K aerospace fiber tensioned within top- and bottom impregnation nano-films. We now have the ability to fully impregnate aerospace composite prepregs with nano-modified prepolymers applicable to wide range of nano-particles, base chemistries, loading levels and areal weights. Aerospace quality 145 gsm prepreg prepared from the 10wt% MWCNT impregnation film is shown in Figure 23.

Figure 22: 10wt% MWCNT nano-matrix film carbon fiber impregnation processing

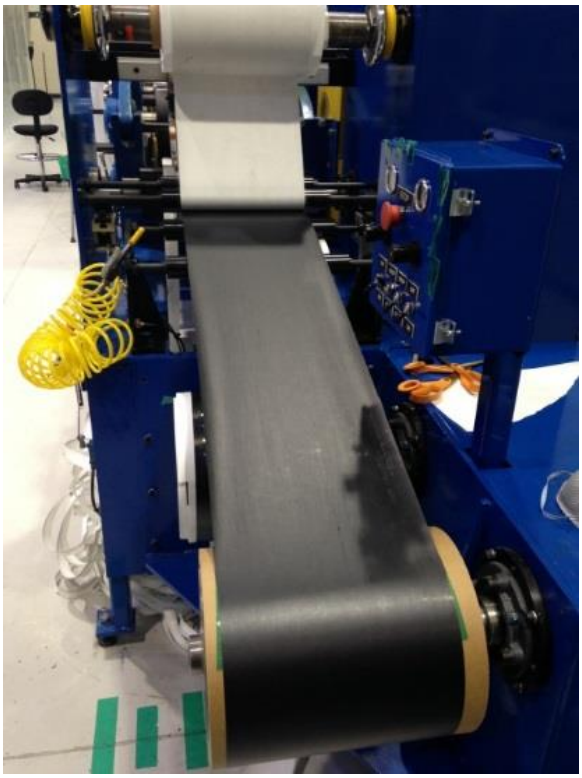

Figure 23: 145 gsm aerospace prepreg prepared from 10wt% MWCNT impregnation film

Interlayering of nanocomposites within aerospace structures is of broad interest to the advanced aerospace and defense communities. In this example, "functional films" are placed onto the surfaces of aerospace prepregs to be incorporated within cured aerospace composite structures as "functional layers". Multi-functional composites can be developed for a broad range of "smart" applications including electrical energy management, thermal energy management, structural health monitoring, signature control, deicing, lightning strike protection, and interlaminar toughening to name a few. In this example, functional films are used as "skin" materials added to the prepreg surfaces prior to lamination and cure of structure. Functional films can be placed onto the single side of aerospace prepreg or both sides of the prepreg. When considering structural performance, functional films can be placed on the top surface (only) of

the composite structure, bottom surface only, single layers at desired placement within a composite structure, or multi-layers which potentially include surfaces and/or throughout the composite structures. Figure 24 shows the process engineering developed during this research for preparing functional skin layers onto the surfaces of prepreg. Figure 24 (left) shows a 15 gsm MWCNT functional layer being placed onto the surface of a standard aerospace 145 gsm prepreg. In this case, we matched the base prepolymer chemistries for the functional layer and prepreg, but it should be noted we have also modified the interlayer prepolymer chemistries from the prepreg for certain applications. Figure 24 (right) shows the 7" functional layer skin on the 12" 145 gsm aerospace prepreg. The process developed from this research provides new pathways for incorporating a broad range of modified functional layers, nanoparticles, loading levels, and chemistries for the advancement of aerospace multifunctional structures.

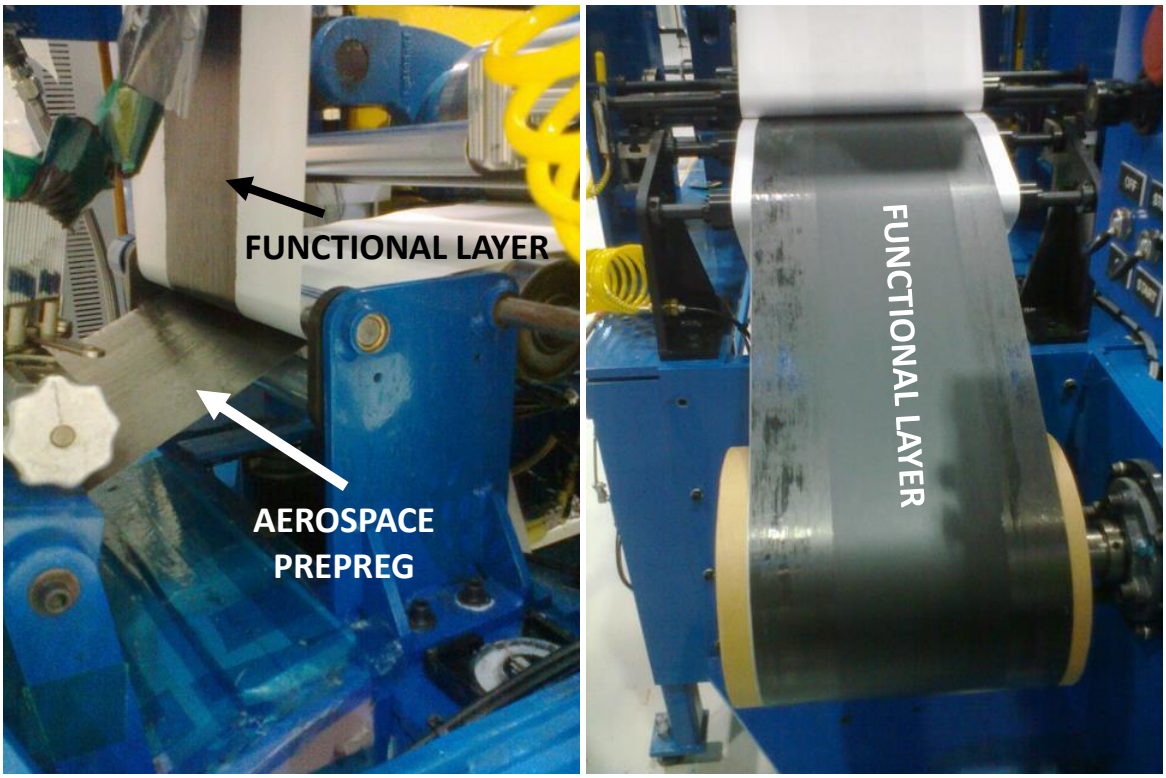

Figure 24: MWCNT functional "skins" on aerospace prepreg materials

Figure 25 shows panel fabrications from MWCNT carbon fiber impregnation and prepreg functional skin materials. A variety of layup configuration including various unidirectional and quasi-isotropic lamination configurations have been fabricated in this research.

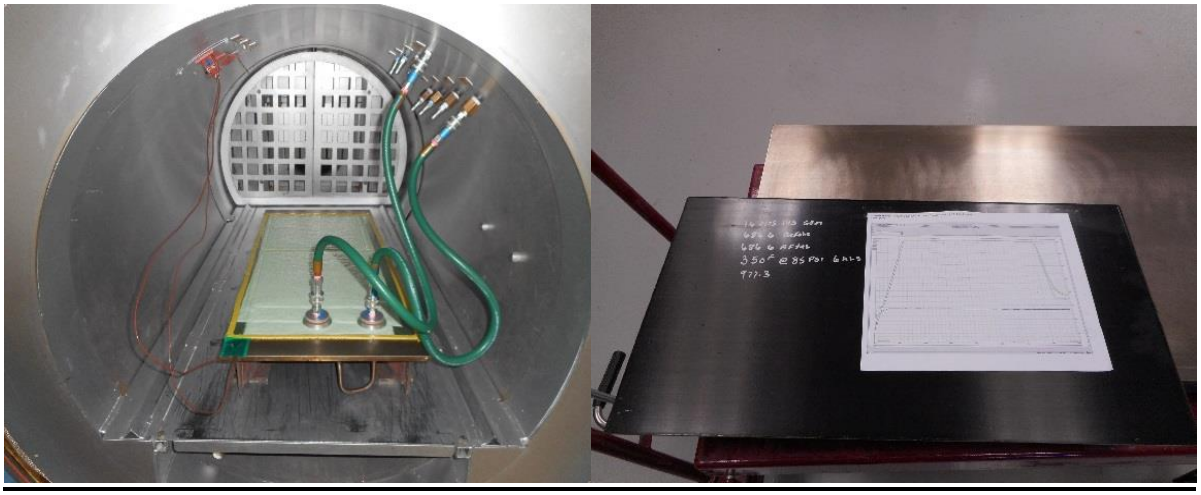

Figure 25: Panel fabrication from MWCNT prepreg and skin materials

Impact of Results

MWCNT nanocomposite aerospace prepregs were successfully prepared through the development of advanced filming and pregregging process technologies. A broad range of aerospace prepolymer base chemistries, nanoparticle chemical compositions/forms, nanoparticle dispersion states and nanoparticle loading levels have been explored and proven throughout this research. Process engineering to prepare pilot scale quantities of 100% solvent free, environmentally favorable, low-cost fully dispersed nanoparticle modified aerospace prepolymers have been proven for:

1. Industrial scale "roll coating processing" for MWCNT prepolymer films ranging from 10 gsm to >40 gsm have been prepared and controlled within aerospace tolerances.
2. Pilot scale "knife-over-plate coating processing" for MWCNT prepolymer films ranging from 15 gsm to >50 gsm have been prepared and controlled within aerospace tolerances
3. Pilot scale MWCNT prepolymer matrix impregnated "prepreg" have been developed at 145 gsm and 190 gsm within aerospace tolerances.
4. Pilot scale MWCNT prepolymer matrix prepreg functional "skins" have been developed at 145 gsm and 190 gsm within aerospace tolerances.

The significance of this work is the demonstration of a rapid development platform for preparing nanocomposites of various configurations into aerospace quality test panels. This comprehensive development platform is capable of fully dispersing nanoparticles into various aerospace matrix chemistries at pilot scale and incorporating those new materials into a broad array of structural configurations for rapid and low-cost analysis. This platform offers the Air Force a unique opportunity to translate advancements learned through a broad research base into a materials development infrastructure for up-scaling and rapid translation into structural analyses.

4. Aerospace Composite Cured Nanostructured Matrix Morphologies Developed

MWCNT nanocomposites have the potential to impart desirable electrical, thermal and mechanical properties to aerospace composite materials, however observed property enhancements depend upon on the aggregation states. The tendency for nanotubes to

agglomerate with to a reduction in matrix viscosity, especially during composite cure, is widely acknowledged. Controlling agglomeration states is an important consideration for the adoption of these materials into aerospace structures. This research has helped our group better understand the relationship between epoxy network architecture for a variety of the epoxy and amine chemistries to study how cure influences MWCNT agglomeration in prepolymers vs. cured/vitrified states. Understanding the role of agglomerate morphology with respect to these attributes will aid the scientific community in further development of nanostructured multifunctional materials. To understand which agglomerate morphologies correlate favorably and directly with certain physical, chemical, thermal, and electrical properties, we have started to develop curing methods which target controlled dispersion states and nanostructured morphologies within cured aerospace matrices. The level of control over cured agglomerate morphologies we have studied will help to gain a fundamental understanding of CNT spatial contributions with nanocomposite performance. Continuation of this work will provide for the development of optimized cure prescriptions to target specific and reproducible nanostructured morphologies and as a result, optimized properties.

Figure 26 depicts the rheological profiles for a nanocomposite prepolymer prepared with 0.1% wt/wt Baytubes cured under two thermal profiles. The 1S cure profile of 180^{o}C for 3 hours since it is a common thermal cure profile for aerospace composites. The viscosity for the 1S sample evolved as a “parabolic well” with a reduction in viscosity associated with increasing temperatures and then followed by a steady increase in viscosity associated with chain extension and conversion leading towards the gel-point. The 2S thermal prescription of 80^{o}C for 3h was developed specifically to eliminate the parabolic well viscosity and exhibit a constant increase in

viscosity towards chemical gelation. In other words, at 80^{o}C we have established a cure condition that advanced viscosity without a rheological well that facilitates re-agglomeration. This stark difference in viscosity profile is important, as it is within the "viscosity well" that nanotubes are mobile and agglomeration is occurs. So the two cure prescriptions provide pathways for agglomeration to occur, or be prevented through control of the rheological states of the matrix polymer. We have determined through this work that the 1S cured drop in viscosity facilitates agglomeration of tubes until a percolated network of nanotubes forms. Analogous to a series of "nano-wires", this network morphology can cause a physical gelation that temporarily locks the morphology in place and arrests agglomeration.

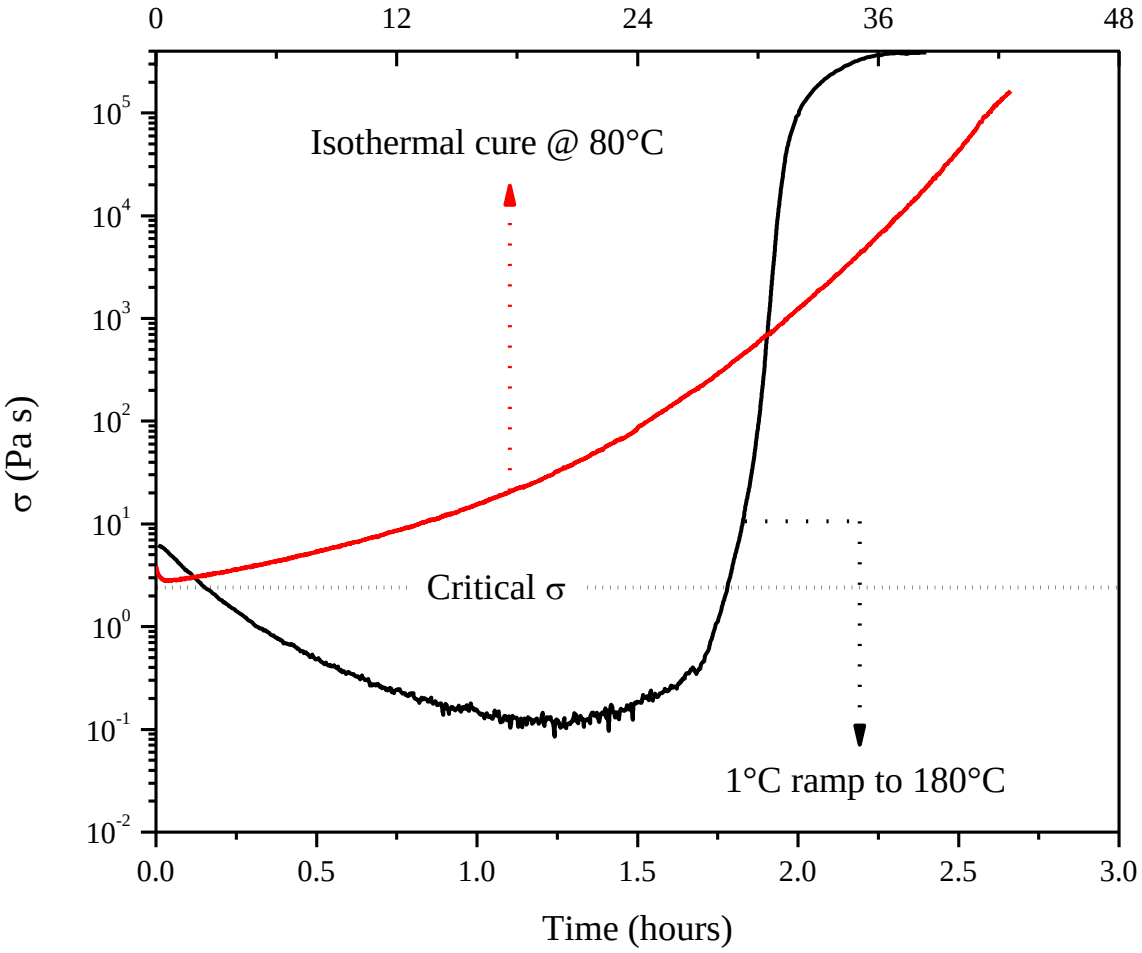

Figure 26: Rheology cure profiles of 0.1% Baytubes dispersed in 44DDS-TGDDM

Nanoparticle dispersion at the micro scale is often used as a representation of the overall dispersion state of a material. We chose to track the effect on agglomeration within these two cure prescriptions using optical microscopy, specifically because the overall sample size was much larger than the average nanotube agglomerate size. Because of this, it was possible to evaluate the development of agglomerate size and morphology which evolves during cure. Figure 27 shows OM images taken of 0.1% Baytube loaded samples before and after cure of both 1S and 2S samples demonstrating their nanotube agglomerate morphologies. Although a

wide range in MWCNT loading level materials were prepared, for OM observation the 0.1% loaded samples specifically were chosen for their more favorable optical clarity compared to higher loaded samples. Above 0.1% loading, increasing nanotube concentration made resolution of individual agglomerates difficult, confounding observation or remarks on agglomerate size or morphology. These agglomerate size and morphology changes were tracked throughout cure as a time lapse capturing the entire agglomeration development. However due to the limitations of presenting this result in a paper, before and after cure images, in Figure , were chosen to highlight the mentioned cure effect. The nanotube agglomerates in the 2S sample remained essentially stationary throughout cure, while the 1S sample developed a nanotube agglomerate morphology resembling a nanowire network. This percolated network type morphology has been reported by Alig, Yourdkhani, Martin, *etc.* in various systems, but not necessarily commented on.[91, 97, 98] In these cases demonstration of a controlled method for dictating morphology state in cured thermoset matrices was absent. Also unreported was a means to leave a maximally dispersed morphology state intact, as observed in the 2S samples of this study. To our knowledge the ability to adjust dispersion morphologies in the cured nanocomposites from aliquots of a single composition has never been reported and is a novel contribution to the field.

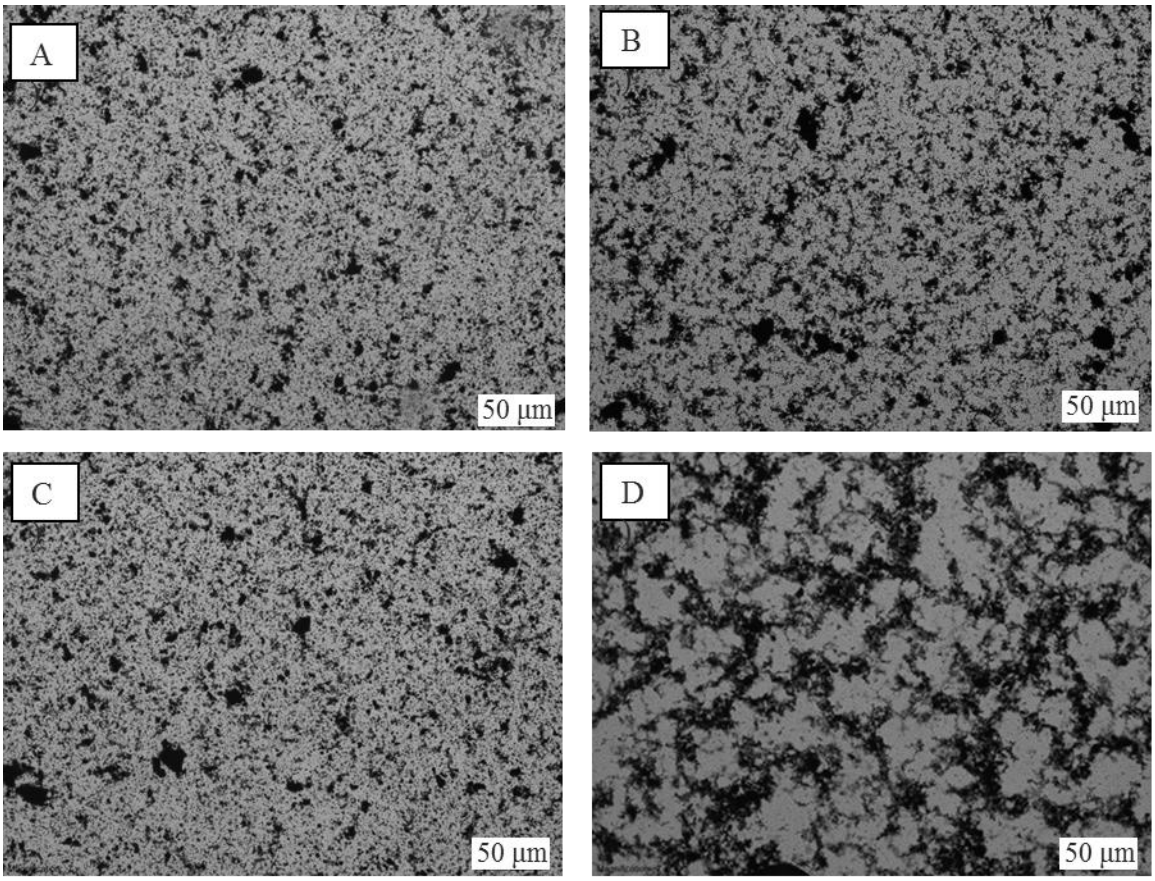

Figure 27: OM images showing nanotube dispersion states for 2S cure profile (A & B) and 1S cure profile (C and D)

Figure 28 presents the in-plane DC conductivity of samples cured under the two prescribed cure conditions and MWCNT contents ranging from 0.02 to 15% wt/wt. The 2S samples exhibited conductivities consistently an order of magnitude lower than the 1S samples at concentrations above percolation threshold, suggesting the formation of "nano-wires" which evolve during re-agglomeration may play a significant role in electrical conductivity. Also, the onset of percolation was shifted from 0.5% to 0.1% wt/wt nanotubes when comparing the 2S to the 1S prescription which indicates the formation of a conductive network much sooner in the 1S samples. The decade shift in conductivity observed between the two cure cycles would suggest a

more efficient percolated network structure being formed within the 1S cured samples. This result can be rationalized through the OM observations discussed for Figure 27. It is also interesting to note that the trend of increased conductivity between the two cure protocols appears to be converge at high loading levels. At low loading levels the nanocomposite rheological response is a matrix dominated property and more temperature dependent. However, at high loading levels material viscosity becomes increasingly dependent on the dispersion state of the MWCNT and therefore less temperature dependence. We hypothesize leading to lower mobility of MWCNT which limits formation of nano-wires and observed gains in conductivity.

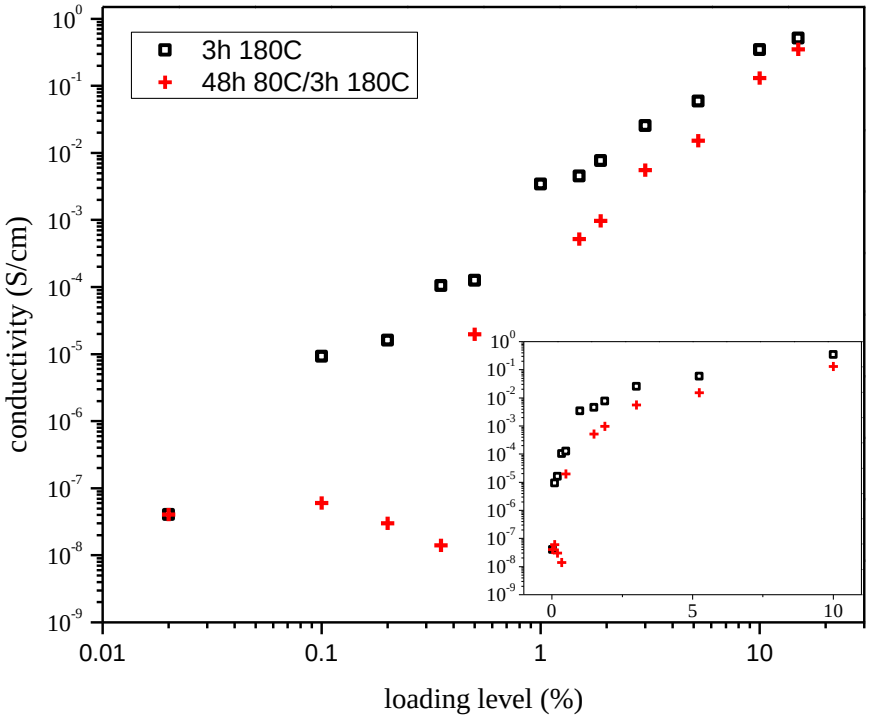

Figure 28. Four point probe conductivity measurements comparing MWCNT loading levels and cure prescriptions

Representative TEM images for 2S and 1S cured MWCNT dispersed at loading levels between 0.1% and 10.0% wt/wt in cured aerospace networks are shown in Figure 29 and

represent typical agglomerate sizes observed at the sub-micron level. Similar to the trends observed in OM, altering the cure prescription appears to result in distinguishing agglomerate content and size-scale across all loading levels. However, the qualitative differences in the spacial arrangement of nanotubes favors the theory that agglomeration during cure is driven by viscosity which leads to the decade shift in bulk conductivity. At the highest loaded levels, namely the 5 and 10% wt/wt, samples begin to appear nearly analogus which agrees with the trends observed in the bulk conductivity measurements previously discused.

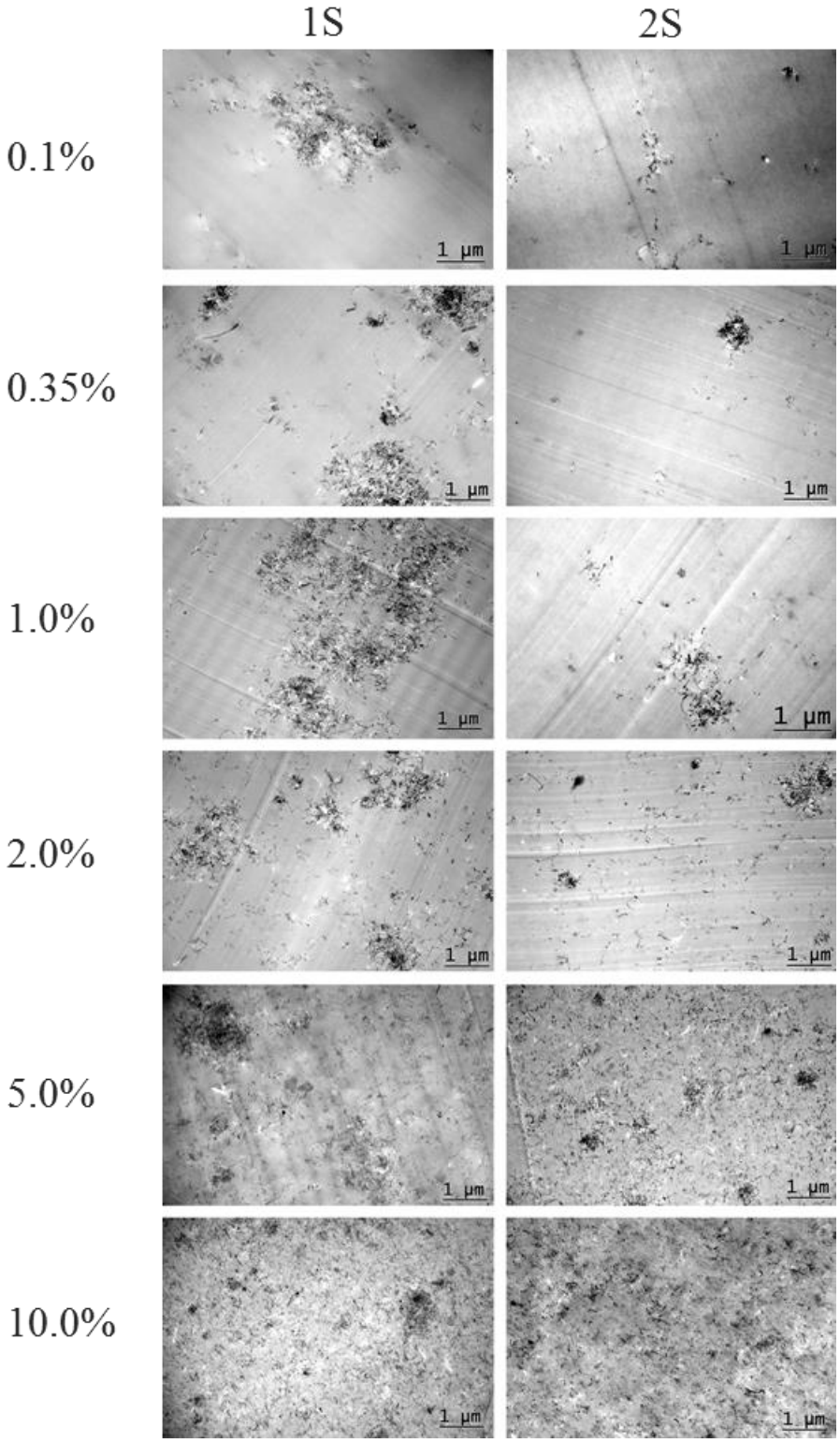

Figure 29. TEM images showing nanotube dispersion after cure for 2S and 1S samples at nanotube loadings between 0.1 and 10.0% wt/wt

Impact of Results

The properties of nanotube modified aerospace matrix networks are clearly dependent upon the agglomeration states and resulting nano-structured morphologies. The effect of the agglomerate morphology develops with cure and final properties. Our findings in this research highlight two important factors which rationalize inconsistencies and on-going debates regarding reported results in our field:

1) The evolutionary pathway towards the cured morphological state is seldom quantified in literature
2) A solvent free preparation method for advancing MWCNT nanocomposites to specific and reproducible prepolymer and cured network morphologies has not been reported.

Our method for controlling MWCNT secondary agglomeration and cured network morphology through controlling the cure prescription and rheological states for aerospace epoxy MWCNT nanocomposites is significant. We showcased two cure prescriptions for our system, but envision numerous pathways for manipulating ultimate nanostructured morphologies and ultimate properties will become the basis of continued research and exploration. The elevated temperature viscosity-well cure profiles which promote the formation of nanowire agglomerates is particularly interesting for advancing energy management within cured aerospace composites. This simple manipulation of network cure profile demonstrates over a decade improvement in both electrical conductivity and percolation threshold through a controlled rheological parabolic-well. In-contrast, applying a modification in cure with elimination of the rheological parabolic-well demonstrated an ability to mitigate MWCNT agglomeration and maintain a fully dispersed morphology. It has become apparent that manipulation of the ultimate nanostructured

morphology in a cured aerospace structure may be necessary to advance desirable properties. For example, the formation of MWCNT cured aerospace epoxy nano-wire morphology may facilitate electrical and thermal energy transport, while a fully dispersed morphology favor mechanical, interlaminar and shear sensitive properties of the cured aerospace networks.

5. Aerospace Composite Benzoxazine Matrix Continuous Reactor Developed

Recent interest in high performance composites has shifted toward a potential alternative thermosetting matrix to the traditional epoxy portfolios, benzoxazines. Benzoxazines are identified by their characteristic oxazine, or heterocyclic, ring containing oxygen and nitrogen, and are considered to couple the thermal and fire retardant properties of phenolics with the modular molecular design of epoxies. This combination renders benzoxazines an attractive matrix chemistry for aerospace composite applications. Although benzoxazine chemistries are desirable for use in aerospace composites, their synthetic preparations and product forms have led to limited utility in aerospace, and the adopted approach to date is blending benzoxazines with epoxies for aerospace materials. Although this approach has utility for preparing new matrix chemistries which employ within the aerospace materials infrastructure, ultimate and desirable properties are sacrificed in the epoxy blend. We have extended the continuous reactor technology developed through our AFOSR research to determine the feasibility of preparing 100% benzoxazine prepolymers through our new reactor technology and which are feasible in aerospace composites environments. Much to our surprise, this research exploration has proven what is now platform from which benzoxazine monomers (BOX-CR) and prepolymers (BOX-PP) can be synthesized in

our continuous, solvent-free, and one-step chemical reactor providing an environmentally-favorable and cost-effective processing method.

Our continuous benzoxazine reactor, depicted in 30, was comprised of a Prism 16 mm co-rotating intermeshing twin-screw high shear chemical reactor (L/D = 25). The screws were enclosed by 5 independent barrels, or zones, which were electrically heated and liquid cooled. The screw configuration was designed to balance high-shear mixing and residence time to promote full conversion of reactants to monomer and/or targeted prepolymer conversion.

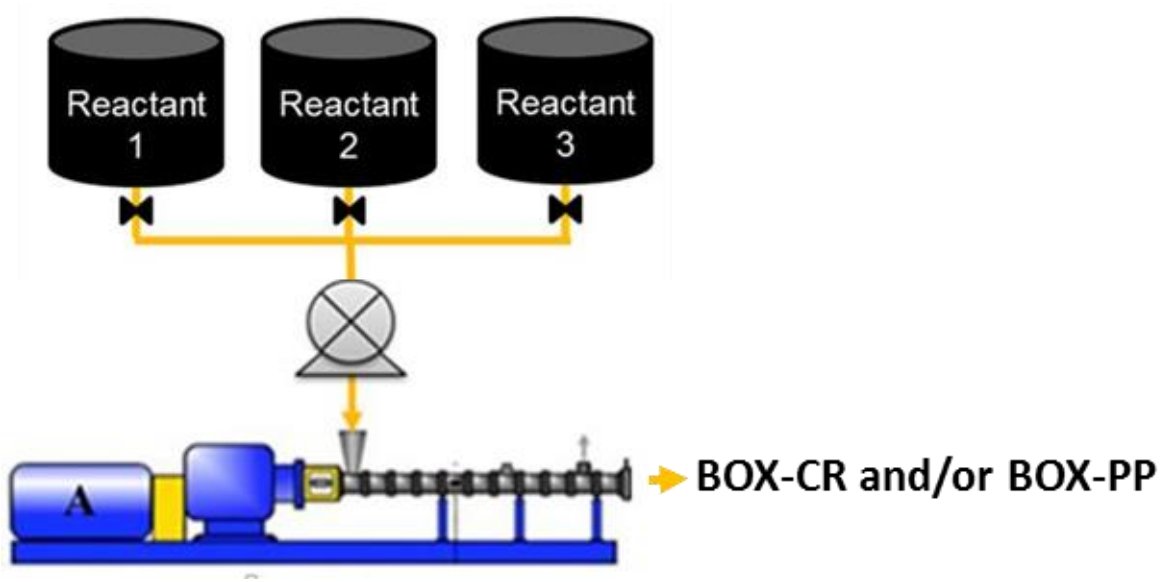

Figure 30. General process design of continuous high-shear reactor.

Structural validations of the synthesized monomers were obtained from ^{1}H NMR characterizations performed in deuterated chloroform ($CDCl_3$) using a Varian Mercury Plus 300 MHz NMR spectrometer operating at a frequency of 300 MHz with tetramethylsilane as an

internal standard. For the integrated intensity determination of the ^{1}H NMR spectra, 32 transients and a relaxation time of 5 s was used. ReactIR spectra and analyses were collected using a Mettler Toledo ReactIR 45M equipped with fiber optic probe and silicon probe tip. Spectral analyses were performed using ICiR software version 4.2, which afforded reaction kinetics characteristics and reaction temperature monitoring in real-time. Sampling was conducted in the range 2800-650 cm^{-1} while acquiring 16 scans at 8 cm^{-1}. Using each reactant and a previously synthesized BOX sample as reference spectra, the ConcITt feature calculated relative concentrations by deconvoluting peaks during the batch reactor synthesis. Prepolymer conversions were determined by DSC analyses.

The reaction scheme of monofunctional benzoxazine (BOX) syntheses depicted in Figure 31 is comprised of reacting any substituted phenol and primary amine and paraformaldehyde in molar ratios of 1:1: ≥ 2, respectively.

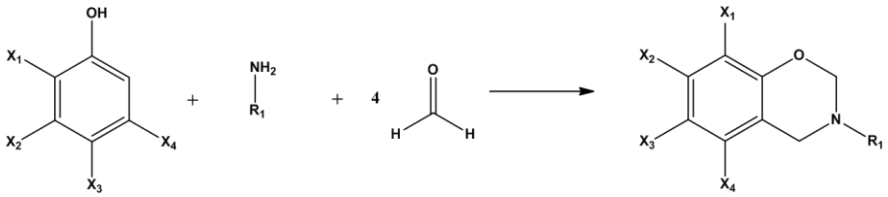

Figure 31. Monofunctional benzoxazine reaction.

In the present synthesis, the meta-substituted phenol yields an isomer blend of monomer **A** and monomer **B** as depicted in Figure 32, where monomer **A** is the major product due to the reduced steric hindrance from the substituent of the phenol.

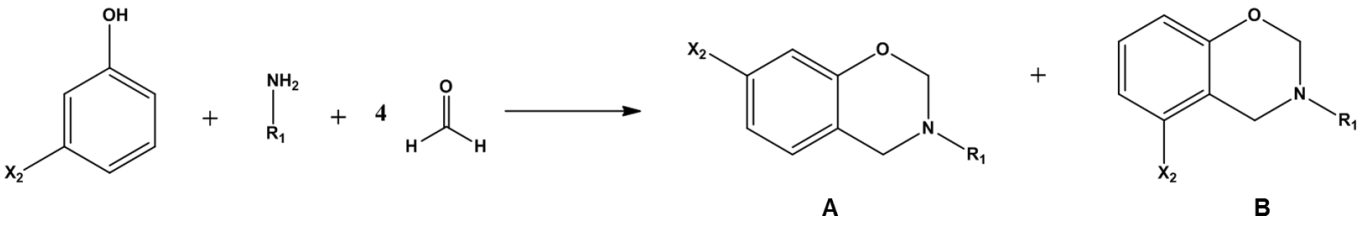

Figure 32. Isomeric product formed in BOX-BR

The absence of solvent in this melt synthesis affords the maximum kinetic efficiency as the collision frequency is high. However, kinetic control is almost impossible because this solventless protocol creates a heterogeneous system in which gas-liquid, liquid-solid, and gas-solid interactions occur.[10] Furthermore, the competition between benzoxazine ring formation and oligomerization constitute a narrow temperature range for processing.

During the synthesis of BOX-BR, ReactIR kinetics data shown in Figure 33 established that the reaction of phenol and paraformaldehyde react faster than the amine and paraformaldehyde. ^{1}H NMR spectra validated that the methylene bridge between the oxygen and nitrogen of the oxazine ring formed first. Increasing the reaction temperature resulted in the formation of the methylene linkage between the nitrogen of the oxazine ring and the benzene ring of the phenol.

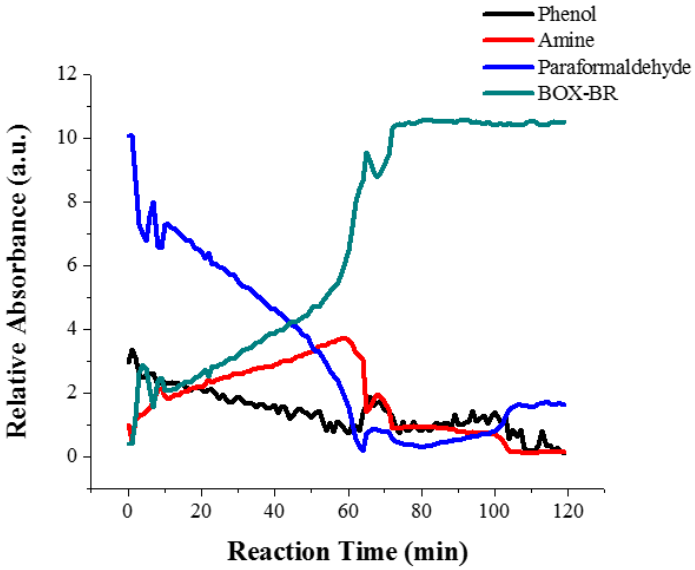

Figure 33. Reaction kinetics of BOX-BR synthesis.

The reaction product contained monomer and oligomer, as expected in the melt method, thus providing the need for purification. The ^{1}H NMR spectrum of the purified product, illustrated in Figure 34, validated that the BOX isomers were successfully synthesized.

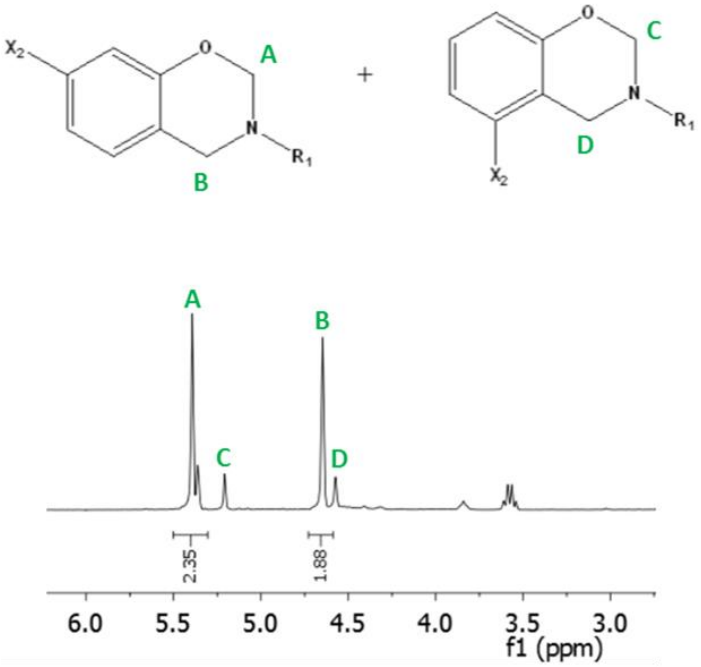

Figure 34. ^{1}H NMR spectrum of purified BOX-BR.

When comparing the integrated values of the characteristic benzoxazine peaks at 5.5 ppm (-O-CH_2-N-) and 4.5 ppm (-N-CH_2-Ar-) of the isomers, it was found that the purified isomer blend was comprised of 80% monomer **A** and 20% monomer **B**.

To provide a direct comparison between a batch reactor and our continuous high-shear reactor methods, the same reagents and molar ratios were used to make the feedstock that was pumped to the inlet of the reactor. Aliquots from each processing temperature were characterized via ^{1}H NMR, which identified the processing temperatures where the methylene bridge between the amine of the oxazine ring and benzene of the phenol (-N-CH_2-Ar-) would not fully form or integrate to 2 protons. However, the temperature at which both of the characteristic benzoxazine peaks integrated to 2 protons indicating the presence of fully ring closed monomer, was identified as depicted in the unpurified NMR spectrum in Figure 35.

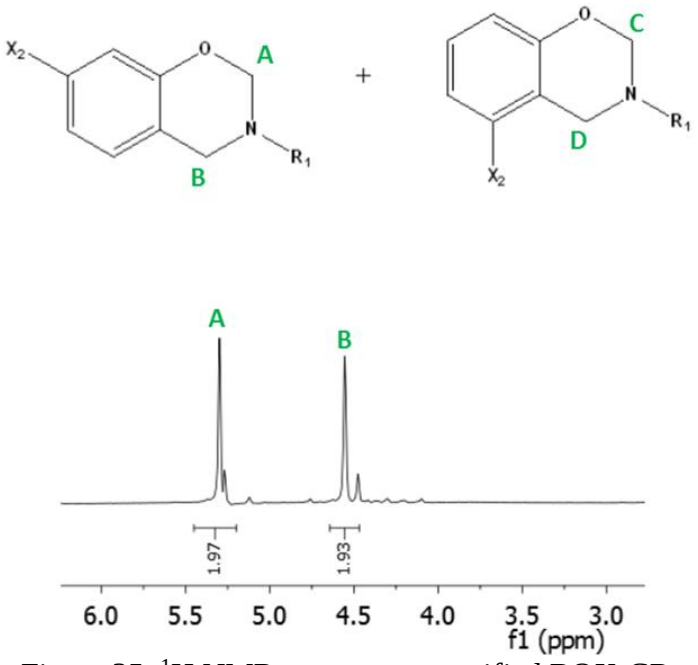

Figure 35 ^{1}H NMR spectrum unpurified BOX-CR.

When comparing the ^{1}H spectra of purified BOX-BR and unpurified BOX-CR, as depicted in Figure 36, the continuous reactor was capable of synthesizing BOX without the need of purification and with reduced monomer **B** content (~12%) in 60 sec as opposed to 120 min to synthesize and purify using a batch reactor.

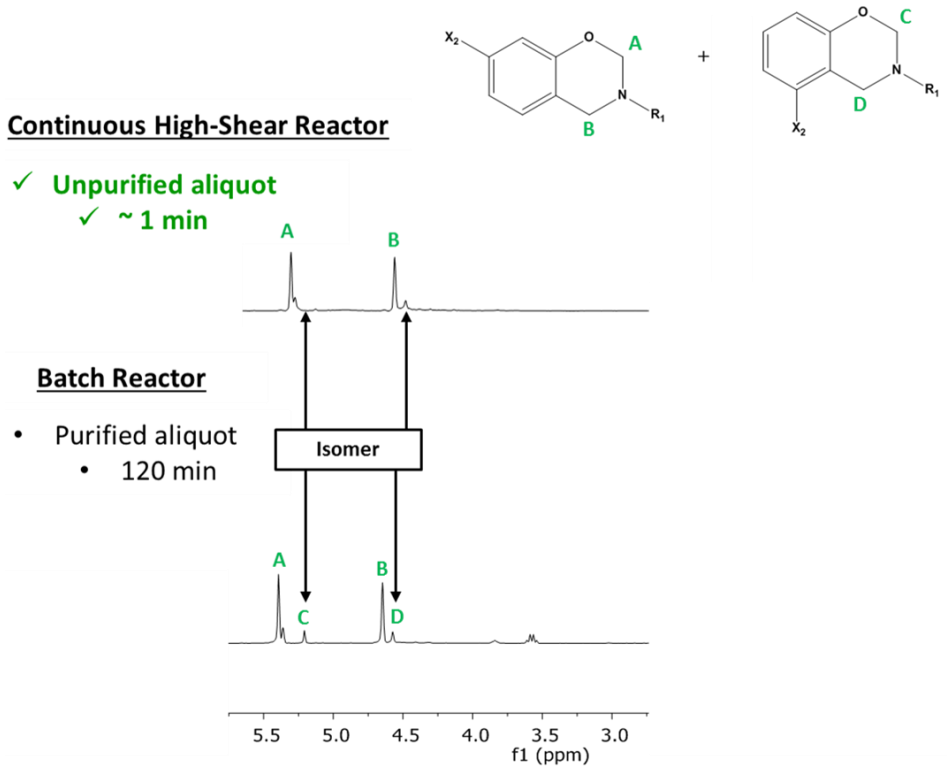

Figure 36. ^{1}H spectra of purified BOX-BR and unpurified BOX-CR.

Although benzoxazine monomers have been reportedly melt synthesized in batch reactors and single-screw extruders, there is no prior work or technology that exhibits the truly

"continuous" and single-step reactor design of the present invention. We hypothesize that the reaction kinetics were increased greater than 100x that of the batch reactor kinetics and increased the reaction efficiency favoring the major isomer due to the reduced reaction volume, increased heat transfer, and high-shear environment in the continuous high-shear reactor. Considering that the continuous high-shear reactor is starve fed and Fick's first law of diffusion (Equation 6):

$$J = -D\frac{\partial \varphi}{\partial x} \qquad \text{Eqn. 6}$$

where J is the diffusion flux with respect to the amount of substance per unit time (mol/m^{2}s), φ is the amount of substance per unit volume (mol/m^3), and x is length (m), the diffusion coefficient is drastically increased since the volume of reagents is reduced and distributed along the barrel of the reactor increasing the reactive surface area. Furthermore, reducing the reacting volume, increasing the physical contact, and having the ability to utilize a reaction temperature above the batch reactor method yields a more homogeneous distribution of reacting phases. Synergistically, these attributes are believed to explain the drastic increase in reaction kinetics and increased reaction efficiency. These explanations are believed to support the broadening NMR peaks as the processing temperature was increased. Peak broadening is a result of ring-opening or polymerization reactions. When the processing temperature was increased, with the addition of a multifunctional monomer, prepolymer conversion increased.

The current technology has been unable to synthesize high-purity benzoxazine monomers in 60 s and has failed to discover the increased efficacy in reaction kinetics that favor the major product, by utilizing the continuous high-shear reactor method reported in this work. Furthermore, the high-purity of the product eliminated the need for post-processing purification. When monofunctional and multifunctional monomers were charged to the reactor, prepolymer conversion increased with as a function of the processing temperature. Synergistically, these attributes significantly increase the throughput and reduce the cost of synthesized benzoxazine monomers and prepolymers.

1.

1. Report Type

Final Report

Primary Contact E-mail

Contact email if there is a problem with the report.

jeffrey.wiggins@usm.edu

Primary Contact Phone Number

Contact phone number if there is a problem with the report

601-266-6960

Organization / Institution name

University of Southern Mississippi

Grant/Contract Title

The full title of the funded effort.

Optimizing Glassy Polymer Network Morphology for Nano-Particle Dispersion, Stabilization and Performance

Grant/Contract Number

AFOSR assigned control number. It must begin with "FA9550" or "F49620" or "FA2386".

FA9550-13-1-0103

Principal Investigator Name

The full name of the principal investigator on the grant or contract.

Jeffrey Stuart Wiggins

Program Manager

The AFOSR Program Manager currently assigned to the award

Dr. Joycelyn Harrison

Reporting Period Start Date

03/01/2013

Reporting Period End Date

02/28/2016

Abstract

MWCNT nanocomposite aerospace prepolymers were successfully prepared in a one-step high volume process through the development of a new preparation approach based upon a high-shear continuous reaction method. The continuous reactor based upon two principle advancements in process engineering.
1. Chain extension prepolymer reactions including curative dissolution, toughener dissolution and controlled chain-extension reactions in the continuous reactor high temperature "hot-zone" to advance conversion, rheology and tack.
2. Simultaneous MWCNT dispersion and stabilization in the continuous reactor low temperature "cold-zone" leading to an increased viscosity and stabilization of MWCNTs within rheological regimes which inhibit re-agglomeration to aid in post processing stabilization of dispersion state through final cure.
The significance of this work is the demonstration of a new method to prepare fully dispersed MWCNT aerospace prepolymers, from reactants to finished products in under 90 seconds reaction time (Figure 19). This reactor technology provides a new pathway for preparing a broad array of aerospace composite matrix prepolymers through simultaneous reaction, mixing and blending of a broad array of co-reactants, modifiers, and nanoparticles. This new approach is a significant advancement in nanoparticle dispersion and stabilization for aerospace composite matrix prepolymers since it is 100% solids, solvent-free, low

energy and more environmentally friendly than any other dispersion technology. The continuous reactor is readily scalable and provides benefits of increased production scale, substantial economic favorability, and modular reactor designs which allow for increased control over prepolymer rheological profiles, low-to-high controlled shear environments and significantly reduced energy consumption.
MWCNT nanocomposite aerospace prepregs were successfully prepared through the development of advanced filming and pregregging process technologies. A broad range of aerospace prepolymer base chemistries, nanoparticle chemical compositions/forms, nanoparticle dispersion states and nanoparticle loading levels have been explored and proven throughout this research. Process engineering to prepare pilot scale quantities of 100% solvent free, environmentally favorable, low-cost fully dispersed nanoparticle modified aerospace prepolymers have been proven for:
1. Industrial scale "roll coating processing" for MWCNT prepolymer films ranging from 10 gsm to >40 gsm have been prepared and controlled within aerospace tolerances.
2. Pilot scale "knife-over-plate coating processing" for MWCNT prepolymer films ranging from 15 gsm to >50 gsm have been prepared and controlled within aerospace tolerances
3. Pilot scale MWCNT prepolymer matrix impregnated "prepreg" have been developed at 145 gsm and 190 gsm within aerospace tolerances.
4. Pilot scale MWCNT prepolymer matrix prepreg functional "skins" have been developed at 145 gsm and 190 gsm within aerospace tolerances.
The significance of this work is the demonstration of a rapid development platform for preparing nanocomposites of various configurations into aerospace quality test panels. This comprehensive development platform is capable of fully dispersing nanoparticles into various aerospace matrix chemistries at pilot scale and incorporating those new materials into a broad array of structural configurations for rapid and low-cost analysis. This platform offers the Air Force a unique opportunity to translate advancements learned through a broad research base into a materials development infrastructure for up-scaling and rapid translation into structural analyses.
The properties of nanotube modified aerospace matrix networks are clearly dependent upon the agglomeration states and resulting nano-structured morphologies. The effect of the agglomerate morphology develops with cure and final properties. Our findings in this research highlight two important factors which rationalize inconsistencies and on-going debates regarding reported results in our field:
1) The evolutionary pathway towards the cured morphological state is seldom quantified in literature
2) A solvent free preparation method for advancing MWCNT nanocomposites to specific and reproducible prepolymer and cured network morphologies has not been reported.
Our method for controlling MWCNT secondary agglomeration and cured network morphology through controlling the cure prescription and rheological states for aerospace epoxy MWCNT nanocomposites is significant. We showcased two cure prescriptions for our system, but envision numerous pathways for manipulating ultimate nanostructured morphologies and ultimate properties will become the basis of continued research and exploration. The elevated temperature viscosity-well cure profiles which promote the formation of nanowire agglomerates is particularly interesting for advancing energy management within cured aerospace composites. This simple manipulation of network cure profile demonstrates over a decade improvement in both electrical conductivity and percolation threshold through a controlled rheological parabolic-well. In-contrast, applying a modification in cure with elimination of the rheological parabolic-well demonstrated an ability to mitigate MWCNT agglomeration and maintain a fully dispersed morphology. It has become apparent that manipulation of the ultimate nanostructured morphology in a cured aerospace structure may be necessary to advance desirable properties. For example, the formation of MWCNT cured aerospace epoxy nano-wire morphology may facilitate electrical and thermal energy transport, while a fully dispersed morphology favor mechanical, interlaminar and shear sensitive properties of the cured aerospace networks.

Distribution Statement

This is block 12 on the SF298 form.

Distribution A - Approved for Public Release

Explanation for Distribution Statement

If this is not approved for public release, please provide a short explanation. E.g., contains proprietary information.

SF298 Form

Please attach your SF298 form. A blank SF298 can be found here. Please do not password protect or secure the PDF The maximum file size for an SF298 is 50MB.

AFD-070820-035.pdf

Upload the Report Document. File must be a PDF. Please do not password protect or secure the PDF . The maximum file size for the Report Document is 50MB.

FA-9550-13-1-0103 Final Report_Jeff Wiggins.pdf

Upload a Report Document, if any. The maximum file size for the Report Document is 50MB.

Archival Publications (published) during reporting period:

i. Molecular scale cure rate dependence of thermoset matrix polymers, Childers, Christopher, Hassan, Mohammad, Mauritz, Kenneth, Wiggins, Jeffrey, Arabian Journal of Chemistry 2016, 9, 206

ii. Semibatch RAFT copolymerization of acrylonitrile and N-isopropylacrylamide: Effect of comonomer distribution on cyclization and thermal stability, Moskowitz, Jeremy and Wiggins, Jeffrey, Polymer 2016, 84, 311

iii. Thermo-oxidative stabilization of polyacrylontirile and its copolymers: Effect of molecular weight, dispersity and polymerization pathway, Moskowitz, Jeremy and Wiggins, Jeffrey, Polymer Degradation and Stability 2016, 125, 76

iv. High Molecular Weight and Low Dispersity Polyacrylonitrile by Low Temperature RAFT Polymerization, Moskowitz, Jeremy, Abel, Brooks, McCormick, Charles, Wiggins, Jeffrey, J. Poly. Sci. Pt.A – Poly Chem, 2016, 54, 553

v. Polymer chain dynamics in epoxy based nanocomposites as investigated by broadband dielectric spectroscopy, Hassan, Mohammad, Tucker, Samuel, Abukmail, Ahmed, Wiggins, Jeffrey, Mauritz, Kenneth, Arabian Journal of Chemistry 2016, 9, 203

vi. Digital image correlation analysis of strain recovery in glassy polymer network isomers, Stephen Heinz, Jianwei Tu, Matthew Jackson, Jeffrey Wiggins, Polymer 2016, 82, 87

vii. Ductile thermoset polymers by controlling network flexibility, Hameed, Nishar, Fox, Bronwyn, Salim, Nisa, Walsh, Tiffany, Wiggins, Jeffrey Chem. Comm. 2015, 51, 9903

viii. Simultaneous reinforcement and toughness improvement in an aromatic epoxy network with an aliphatic hyperbranched POSS epoxy modifier, Jin, Qingfen, Misasi, John, Wiggins, Jeffrey, Morgan, Sarah ", Polymer, 2015 73, 174

ix. Phenylene ring motions in isomeric glassy epoxy networks and their contributions to thermal and mechanical properties, Tu, Jinwei, Tucker, Samuel, Christensen, Stephen, Sayed, Abdelwahed, Jarrett, William, Wiggins, Jeffrey, 2015 Macromolecules, 48(6), 1748

x. Surface composition control via chain end segregation in polyethersulfone solution cast films, Knauer, Katrina, Greenhoe, Brian, Wiggins, Jeffrey, Morgan, Sarah 2015 Polymer, 57(28), 88

xi. Laser-induced thermo-oxidative degradation of carbon nanotube/polypropylene nanocomposites, Bartolucci, Stephen, Supan, Karen, Warrender, Jeffrey, Davis, Christopher, La Beaud, Lawrence, Knowles, Kyler, Wiggins, Jeffrey 2014 Composites Science and Technology, 105, 166

xii. Continuous reactor preparation of thermoplastic modified epoxy-amine prepolymers, Cheng, Xiaole, Wiggins, Jeffrey 2014 Polymer International, 63(10) 1777

xiii. Thermal stability of polypropylene-clay nanocomposites subjected to laser pulse heating Bartolucci, Stephen, Supan, Karen, Wiggins, Jeffrey, LaBeaud, Lawrence, Warrender, Jeffrey 2013 Polymer Degradation and Stability 98(12) 2497

xiv. Effect of Molecular Weight and Polydispersity on Thermal Ring-Closing Stabilization (Cyclization) of Polyacrylonitrile. Katelyn Cordell, Jeremy Moskowitz, Jeffery Wiggins, Society for the Advancement of Material and Process Engineering, CAMX International Symposium Proceedings, Dallas, TX, October 2015

xv. Dispersion of MWCNTs in an Epoxy Prepolymer Matrix Via Continuous Reactor Processing. Andrew Frazee, Jeffrey Wiggins, Society for the Advancement of Material and Process Engineering, CAMX International Symposium Proceedings, Dallas, TX, October 2015
xvi. Quantitative Analysis of the Effect of Ramp Rate on Network Formation during the Cure of TGDDM-DDS Matrices Using Near-Infrared Spectroscopy. Andrew Janisse, Jeffrey Wiggins, Society for the Advancement of Material and Process Engineering, CAMX International Symposium Proceedings, Dallas, TX, October 2015
xvii. Effect of Epoxy Molecular Weight on Incorporation of Polyhedral Oligomeric Silsesquioxane (POSS) as Pendant cage in Epoxy-POSS Hybrid Networks. Amit Sharma, Jeffery Wiggins, Society for the Advancement of Material and Process Engineering, CAMX International Symposium Proceedings, Dallas, TX, October 2015
xviii. Manipulation of cure prescription to alter nano-morphology of dispersed multiwall carbon nanotubes. Brian Greenhoe, Jeffrey Wiggins, Society for the Advancement of Material and Process Engineering, CAMX International Symposium Proceedings, Dallas, TX, October 2015
xix. Observing Residual strains in carbon fiber composites laminates with digital image correlation. Kyler Knowles, Jeffrey Wiggins, Society for the Advancement of Material and Process Engineering, CAMX International Symposium Proceedings, Dallas, TX, October 2015 (2nd Place Technical Recognition)
xx. Improving Polymer Composite Matrix Toughness with POSS-Modified Hyperbranched epoxies. John Misasi, Sarah Morgan, Jeffrey Wiggins, Society for the Advancement of Material and Process Engineering, CAMX International Symposium Proceedings, Dallas, TX, October 2015
xxi. Improcessabilty of Thermoplastic PEEK composites via Ring Opening Polymerization. Matthew Patterson, John Misasi, Jeffrey Wiggins, Russell Varley, Society for the Advancement of Material and Process Engineering, CAMX International Symposium Proceedings, Dallas, TX, October 2015
xxii. Development of Layered POSS Epoxy-Amine Nanocomposites for Protective Coatings
Jessica Piness, Jeffrey Wiggins, CAMX 2015, Dallas, TX October 2015
xxiii. Atomic Oxygen Exposure Testing of Novel Layered POSS Thermoset Nanocomposites
Jessica Piness, Katrina Knauer, Jeffrey Wiggins, International Astronautical Congress, Jerusalem, Israel, October 2015
xxiv. Ultraviolet Exposure Testing of Novel POSS-Cerium Oxide Thermoset Nanocomposites
Jessica Piness, Katrina Knauer, Jeffrey Wiggins, AIAA Space, Pasadena, CA August 2015
xxv. Atomistic and Macro-scale Mechanical Property Testing of POSS Nanocomposites for Space Applications Jessica Piness, Katrina Knauer, Jeffrey Wiggins, SAMPE Tech 2015, Baltimore, MD, May 2015
xxvi. Cure behavior and polymer chain dynamics of octaphenyl poss-epoxy-amine networked systems via dielectric spectroscopy and dynamic mechanical analysis techniuqes, Jessica Piness, Mohamed Hassan, Jeffrey Wiggins, Society for the Advancement of Material and Process Engineering, International Symposium Proceedings, Orlando, FL, October 2014
xxvii. Controlled polyacrylonitrile precursor chemistries, Jeremy Moskowitz, Brooks Abel, Charles McCormick, Jeffrey Wiggins, Society for the Advancement of Material and Process Engineering, International Symposium Proceedings, Orlando, FL, October 2014
xxviii. Dispersion and stabilization of MWCNT in epoxy prepolymer matrix using continuous reactor, Xiaole Cheng, Brian Greenhoe, Mohamed Hassan, Jeffrey Wiggins, Society for the Advancement of Material and Process Engineering, International Symposium Proceedings, Orlando, FL, October 2014
xxix. Exploring MWCNTs agglomerate morphology control in epoxy matrix for gains in electrical properties, Brian Greenhoe, Xiaole Cheng, Jeffrey Wiggins, Society for the Advancement of Material and Process Engineering, International Symposium Proceedings, Orlando, FL, October 2014
xxx. Network formation dependence on polymer matrix cure rate, Christopher Childers, Mohammed Hassan, Jeffrey Wiggins, Society for the Advancement of Material and Process Engineering, International Symposium Proceedings, Seattle, WA, June 2014
xxxi. Network conversion studies of poss-epoxy-amine nanocomposites, Jessica Piness, Jeffrey Wiggins, Society for the Advancement of Material and Process Engineering, International Symposium Proceedings, Seattle, WA, June 2014

Changes in research objectives (if any):

NA

Change in AFOSR Program Manager, if any:

NA

Extensions granted or milestones slipped, if any:

NA

AFOSR LRIR Number

LRIR Title

Reporting Period

Laboratory Task Manager

Program Officer

Research Objectives

Technical Summary

Funding Summary by Cost Category (by FY, $K)

	Starting FY	FY+1	FY+2
Salary			
Equipment/Facilities			
Supplies			
Total			

Report Document

Report Document - Text Analysis

Report Document - Text Analysis

Appendix Documents

2. Thank You

E-mail user

May 20, 2016 16:38:08 Success: Email Sent to: jeffrey.wiggins@usm.edu